Electronic Excitations and Stability of the Ground State of C_{60} Molecules

F. Bechstedt,[1,2] M. Fiedler,[2] and L.J. Sham[1]
[1] *Department of Physics, University of California San Diego, La Jolla, California 92093 -0319*
[2] *Institut für Festkörpertheorie und Theoretische Optik, Friedrich-Schiller-Universität, 07743 Jena, Germany*
(February 1, 2008)

arXiv:cond-mat/9807144v1 9 Jul 1998

A model study of the singlet excitons in the C_{60} molecule with emphasis on the Coulomb interaction between excited electron and hole leads to a physical understanding of the interaction effects on the absorption spectra and to a new identification of the forbidden excitons in the third-harmonic generation spectra. These conclusions may be tested experimentally on the model predictions related to the optical Kerr effect. The model shows that, with sufficiently strong interatomic than onsite interaction, a T_{2G} exciton could have very low energy or become unstable against the closed-shell ground state. Properties of these interesting cases beyond the C_{60} are briefly examined.

78.66.Tr, 71.20.Tx, 78.40.Ri

I. INTRODUCTION

Since the discovery of C_{60}[1], several experimental and theoretical studies have suggested that undoped and doped solid C_{60} are strongly correlated electron systems. The observational basis includes the unusually high superconducting transition temperature of the alkali-metal-doped fullerites[2], the existence of soft ferromagnetism[3], and the strong Coulomb interaction effects in the Auger, direct and inverse photoemission spectra[4]. The theoretical motivation is based on the narrow bandwidth compared to the strong intra-molecular interaction. This naturally leads to theories based on the Hubbard model with onsite interaction on every carbon atom[4–6]. Strong correlation is used to find a mechanism for superconductivity[7]. Parity doublets of the lowest unoccupied molecular orbitals (LUMO's) of the C_{60} molecule are used for the pairing mechanism[8]. Coulomb interaction of the electrons within a single C_{60} molecule has also taken into account through configuration interaction by several quantum-chemistry calculations[9–12]. On the other hand, quasiparticle correction[13,14] to the local density approximation[15,16] leads to the conclusion that, while the correlation effect is large, the electronic structure in C_{60} is nonetheless that of a standard band insulator[14]. Similarly, the superconducting transition temperature of the alkali-doped C_{60} has been explained by the usual phonon mechanism[17,18].

A common feature among the theories mentioned above is the assumption of the closed-shell ground state for C_{60} with the set of highest occupied molecular orbitals (HOMO's) of symmetry h_u and h_g and the set of LUMO's of symmetry t_{1u} and t_{1g}. We ask the question whether such a ground state is stable against the excitation of an electron from a HOMO to a LUMO. If not, the new ground state would lead to low-lying excited states of a quite different nature. In this paper, we use the C_{60} molecule as a paradigm for molecular solids to investigate the stability of the closed shell ground state. By using a simple model, we hope to understand the factors governing such instability and to explore consequences, such as in nonlinear optical properties. Even if the excited states are only low in energy without causing any instability, they could play an interesting role in some properties, especially superconductivity. The method of this study may be applied to molecular solids and quantum dots besides C_{60}.

First, we address the energy ordering of the closed-shell state and the one electron-hole pair excited states. Shirley et al.[19] used a molecular orbital model to make a comprehensive study of the exciton energy spectrum in solid C_{60}. We adopt a similar approach but use further simplifications. We restrict our attention to a single C_{60} molecule since in the solid the weak overlapping between the molecules[20] would not qualitatively affect our results. We use a nearest-neighbor tight-binding model for the one-electron π orbitals[8,21,22] with the help of symmetry considerations[23]. The essential results of this model are given in Sec. II. In Sec. III, the energies of the electron-hole pair states relative to the closed-shell state are determined in terms of the single-particle energies and the Coulomb interaction. The interaction terms include direct electron-hole attraction and the exchange counterpart[24], interaction on the same carbon site as well as between any pairs of carbon sites in the same C_{60} molecule. The dependence of the pair-state energies on three model parameters, the nearest-neighbor hopping energy V, the intrasite interaction U (including both the direct and exchange contributions) and the typical long-range interaction term $e^2/(\epsilon R_0)$ taking into account the intersite screening effect ϵ and setting the distance scale at the radius of the buckyball, R_0 (≈ 3.5 Å) is discussed. We find that a scenario of either the closed-shell state or an electron-hole pair state being the lowest energy state is possible for reasonable values of the three parameters. The consequences of both scenarios on the linear and nonlinear optical properties are then considered in Sec. IV. Our calculations of the linear optical spectra are compared with experiment and our calculations

of the nonlinear properties are used to suggest measurements which will clarify the situation. Sec. V discusses the results of our work with regard to the nature of the ground state of C_{60}. Our tentative conclusion is that the comparison of the theoretical and experimental linear optical spectra favors the closed-shell state as the ground state. However, there are some unsatisfactory features. We believe that the electro-optic and nonlinear optical measurements can clarify the situation. We speculate on the possibility of molecules with an excitonic state as the ground state.

II. SINGLE-PARTICLE EXCITATIONS

Since one objective of this work is the study of the stability of the closed-shell ground state against the low-lying excited electron-hole pair states, the first order of business is to construct the most relevant one-electron orbitals in C_{60}, namely the HOMO's and LUMO's. Their approximation by π orbitals seems to be well established for low-energy excitations. For instance, the weights of the radial orbital for the h_u and t_{1u} states were about 98% and 95%, respectively, according to Laouini et al.[25]. In the discussion of the electron-hole interaction the small σ-contributions may be negligible. The tight-binding Hamiltonian with nearest-neighbor hopping may be built from the molecular π orbitals[23]:

$$\phi_{lmp}(\mathbf{x}) = N_l \sum_g e_{lmp}(\mathbf{g}) \chi\left(\mathbf{x} - R_0\mathbf{g}\right) \tag{2.1}$$

where $\chi(\mathbf{x} - R_0\mathbf{g})$ is the component of the p wave function centered around the atomic sites $R_0\mathbf{g}$ pointing along the radial direction. We have neglected the difference in bond lengths of the inequivalent bonds. N_l gives the normalization of the molecule state. The quantum number l is used to index the irreducible representations[26] of the icosahedral group I_h, the symmetry group of the buckyball, namely a, t_1, h, t_2, and g, with degeneracies 1, 2, 5, 3, and 4, respectively. The quantum number m runs over the degenerate states of each irreducible representation. The quantum number p denotes the parity of the state. Its introduction indicates that the full symmetry group of C_{60} is $I_h \times Z_2$, where Z_2 is the two-element group consisting of the inversion operator and the identity. The coefficients for different sites may be related to each other by[8]

$$e_{lpm}(\mathbf{g}) = \sum_{m'=-l}^{+l} D^{l^*}_{mm'}(\omega_g) e_{lpm'}(\mathbf{e}), \tag{2.2}$$

where ω_g is the rotation bringing the radial vector from atomic site $\mathbf{e}$ (see Fig. 1, not to be confused with the coefficients $e_{lmp}(\mathbf{g})$) to site $\mathbf{g}$. For the regular three- and five-dimensional representations ($l = 1, 2$) under consideration the $(2l+1) \times (2l+1)$ matrices $\hat{D}^l$ are simply the standard transformation matrices in a rigid body, the so-called Wigner-D functions[27].

The irreducible representations $D^l_{mm'}(\omega_g)$ of the coefficients $e_{lmp}(\mathbf{g})$ reduce the nearest-neighbor Hamiltonian in units of the hopping parameter $-V$ to a set of Hamiltonians given by[8]:

$$h^l_{mm'} = \sum_{i=1}^{3} D^{l^*}_{mm'}\left(\omega_{f_i}\right), \tag{2.3}$$

where the i-sum only runs over the three nearest neighbors $\mathbf{f}_i$ of the site $\mathbf{e}$. The spin degrees of freedom are understood. For readers interested in generating the irreducible representations[27], we record the coordinates $\mathbf{e} = \frac{1}{3}\frac{R}{R_0}(\sin(2\Theta_0), 0, 2 + \cos(2\Theta_0))$, where the angle $2\Theta_0 = \cos^{-1}(1/\sqrt{5})$ is defined by the geodesic arc between two neighboring vertices of the icosahedron. The rotations to the nearest neighbors, $\mathbf{f}_i$, from the atom at $\mathbf{e}$ can be given by the Euler angles $(\alpha = 0, \beta = 2\Theta_0, \gamma = \pi)$, $(\alpha = 2\pi/5, \beta = 0, \gamma = 0)$, and $(\alpha = -2\pi/5, \beta = 0, \gamma = 0)$, respectively for $i = 1, 2, 3$.

The LUMO's and HOMO's of interest belong to the representations t_1 and h respectively, which are isomorphous to the spherical harmonics $l = 1$ (p wave), and $l = 2$ (d wave). The state degeneracy is then $2l + 1$ and the normalization $N_l = \sqrt{(2l+1)/60}$. The corresponding Hamiltonians for these states are

$$\hat{h}^1 = \begin{pmatrix} -1 + \frac{2}{\sqrt{5}} & -\sqrt{\frac{2}{5}} & -\frac{1}{2}\left(1 - \frac{1}{\sqrt{5}}\right) \\ -\sqrt{\frac{2}{5}} & 2 + \frac{1}{\sqrt{5}} & \sqrt{\frac{2}{5}} \\ -\frac{1}{2}\left(1 - \frac{1}{\sqrt{5}}\right) & \sqrt{\frac{2}{5}} & -1 + \frac{2}{\sqrt{5}} \end{pmatrix},$$

$$\hat{h}^2 = \begin{pmatrix} -\frac{1}{5} - \frac{2}{\sqrt{5}} & \frac{1}{\sqrt{5}} + \frac{1}{5} & \frac{\sqrt{6}}{5} & \frac{1}{\sqrt{5}} - \frac{1}{5} & \frac{3}{10} - \frac{1}{2\sqrt{5}} \\ \frac{1}{\sqrt{5}} + \frac{1}{5} & -\frac{1}{5} + \frac{2}{\sqrt{5}} & -\frac{\sqrt{6}}{5} & -\frac{3}{10} - \frac{1}{2\sqrt{5}} & -\frac{1}{\sqrt{5}} + \frac{1}{5} \\ \frac{\sqrt{6}}{5} & -\frac{\sqrt{6}}{5} & \frac{9}{5} & \frac{\sqrt{6}}{5} & \frac{\sqrt{6}}{5} \\ \frac{1}{\sqrt{5}} - \frac{1}{5} & -\frac{3}{10} - \frac{1}{2\sqrt{5}} & \frac{\sqrt{6}}{5} & -\frac{1}{5} + \frac{2}{\sqrt{5}} & -\frac{1}{\sqrt{5}} - \frac{1}{5} \\ \frac{3}{10} - \frac{1}{2\sqrt{5}} & -\frac{1}{\sqrt{5}} + \frac{1}{5} & \frac{\sqrt{6}}{5} & -\frac{1}{\sqrt{5}} - \frac{1}{5} & -\frac{1}{5} - \frac{2}{\sqrt{5}} \end{pmatrix} \tag{2.4}$$

where $\cos(2\Theta_0) = 1/\sqrt{5}$ and $\cos(\frac{2\pi}{5}) = \frac{1}{4}(-1 + \sqrt{5})$ are used.

The eigenvalues λ of the reduced Hamiltonians for the two LUMO and two HOMO levels are, for $l = 1$,

$$\begin{aligned} \lambda_{1+} &= \frac{1}{2}(-3 + \sqrt{5}), \\ \lambda_{1-} &= \frac{1}{2}[(3 + \sqrt{5})/2 - \sqrt{(19 - \sqrt{5})/2}], \end{aligned} \tag{2.5}$$

and for $l = 2$,

$$\begin{aligned} \lambda_{2-} &= \frac{1}{2}(-1 + \sqrt{5}), \\ \lambda_{2+} &= 1, \end{aligned} \tag{2.6}$$

in agreement with other calculations[8,22,23]. These orbitals are associated, respectively, with the symmetry t_{1g}, t_{1u}, h_u, and h_g. The single-particle energies of these molecule states are

$$\varepsilon_{lp} = -\lambda_{lp} V, \tag{2.7}$$

where lp runs over the indices $1+$ (for the representation t_{1g}), $1-$ (t_{1u}), $2-$ (h_u), and $2+$ (h_g).

For these parity doublets with not so very different energies, the Hamiltonians (2.4) give the normalized eigenvectors with $(2l+1)$ components (with $x = \lambda_{1-} - 2 - \frac{1}{\sqrt{5}}$ and $\tan y = \sqrt{5}x/2$) at carbon site $\mathbf{e}$ as

$$\hat{e}_{1+}(\mathbf{e}) = \frac{1}{\sqrt{2}} \begin{pmatrix} 1 \\ 0 \\ 1 \end{pmatrix}, \quad \hat{e}_{1-}(\mathbf{e}) = \frac{1}{\sqrt{2}} \begin{pmatrix} -\sin y \\ \sqrt{2}\cos y \\ \sin y \end{pmatrix},$$

$$\hat{e}_{2-}(\mathbf{e}) = \frac{1}{\sqrt{10}} \begin{pmatrix} 1 \\ 2 \\ 0 \\ 2 \\ -1 \end{pmatrix}, \quad \hat{e}_{2+}(\mathbf{e}) = \frac{1}{\sqrt{30}} \begin{pmatrix} -1+\sqrt{5} \\ 1+\sqrt{5} \\ \sqrt{6} \\ -1-\sqrt{5} \\ -1+\sqrt{5} \end{pmatrix}, \tag{2.8}$$

triplets for the LUMO states and quintets for the HOMO states. The complete eigenvectors with the components for the other atoms follow by rotation (2.2). Using this equation, the definition of the Wigner-D functions[27], and the form of the vectors in Eq. (2.8) one can easily show the parity of the states, $e_{lm\pm}(-\mathbf{g}) = \pm e_{lm\pm}(\mathbf{g})$. The pairs of vectors for the atoms at the sites $\mathbf{e}$ and $-\mathbf{e}$ give instructive examples. The corresponding transformation matrices $D^l_{mm'}(0,\pi,0) = (-1)^{l+m}\delta_{m,-m'}$ gives eigenvectors at $-\mathbf{e}$, which fulfill the parity condition. Since the rigid-body transformation from $\mathbf{e}$ to $-\mathbf{g}$ may be related to a product of transformations from $\mathbf{e}$ to $\mathbf{g}$ and $\mathbf{e}$ to $-\mathbf{e}$, the above property is also valid for arbitrary atomic positions $\mathbf{g}$.

Fig. 2 shows schematically the two LUMO levels and two HOMO levels and their associated states. The energy scale is set by the hopping matrix element V in Eq. (2.7). The single-particle energy difference $(\varepsilon_{1-} - \varepsilon_{2-})$ is taken to be 3.5 eV between t_{1u} and h_u peaks in solid C_{60} measured by the photoemission and inverse-photoemission experiments[4,28,29]. This yields an estimate of $V = 4.626$ eV. The brackets $V = (3.83, 6.61)$ eV represent the uncertainty of this estimate. The lower value arising out of the finite band widths is taken to be the midpoint between the band onset at 2.3 eV[4] and the peak-to-peak difference at 3.5 eV. The higher value of V comes from the estimate of 5 eV as the difference between the electron affinity level and the ionization potential of the C_{60} molecule[30]. The three values of V yield the single-particle excitation spectrum $\varepsilon_{1+} = 4.63$ (3.83, 6.61) eV (t_{1g}), $\varepsilon_{1-} = 3.50$ (2.90, 5.00) eV (t_{1u}), $\varepsilon_{2-} = 0$ eV (h_u), and $\varepsilon_{2+} = -1.77$ (-1.46, -2.52) eV (h_g) with respect to the position of the highest occupied state. The discrepancy between these values of V and the LDA derived $V = 2.72$ eV[25] represents the phenomenological fit of the former to the renormalized one-particle energies so that, when the interaction between two single-particle excitations is considered later, the one-particle energies should not be further modified by the interaction.

III. EXCITONS

A. Symmetry-adapted electron-hole pair states

In this paper, we shall consider only electron-hole excitations without spin flip, i.e. only singlet excitons. We have calculated the energies of the triplet excitons, which, devoid of exchange interaction terms, lie slightly lower than the singlets[19]. The possibility of magnetism involving the triplet state will be left to a future study.

Consideration of the electron-hole pair excitations of the π-electron system of C_{60}, which are lowest in energy, can be restricted to the level scheme of Fig. 2 with the empty levels t_{1g} and t_{1u} and the occupied states h_u and h_g. The pair excitations contain products of the type $t_{1p_e} \times h_{p_h}$ with the single-particle parities $p_e, p_h = +1$ (g) or $= -1$ (u). With the pair parity $P = p_e \cdot p_h$, where P runs over the same values $+1$ (G) and -1 (U) as p_e and p_h, the pair states have the symmetry[10]

$$t_{1p_e} \times h_{p_h} = T_{1P} + T_{2P} + G_P + H_P. \tag{3.1}$$

That is, each of these four 15-dimensional product representations of a singlet electron-hole pair from LUMO/HOMO of the type $h_{p_h} \rightarrow t_{1p_e}$ splits up into two three-dimensional representations, T_{1P} and T_{2P}, one four-dimensional G_P representation and one five-dimensional H_P representation ($P = G, U$)[31]. Among them is the dipole-allowed pair excitations T_{1U} for electron and hole with opposite parity. For these optically observable excitons, there is no need to consider the four-fold degenerated g_g hole level which is either somewhat below the h_g level[10] or degenerate with it within the approximations considered[8,22,23], from the relation[10]

$$t_{1p_e} \times g_g = T_{2P} + G_P + H_P, \tag{3.2}$$

which contains no representation T_{1U} of the electric-dipole-allowed excitons. Symmetry reasons also dictate that there is no configurational interaction between the A_G ground state and the low-lying pair states considered.

We develop a method of computing the excitonic states in terms of the symmetry-adapted electron-hole pair states (and incidentally gained some physical insight into these pair states) by exploiting the close relation of the representations of the symmetry group I_h of the C_{60} molecule with the transformation properties of the spherical harmonics[23] which differ by a small perturbation. The (t_{1p_e}) of the LUMO and the (h_{p_h}) of the HOMO correspond to single-particle angular momentum

states with the quantum numbers l and m ($l = 1, 2$ and $-l \le m \le l$). The angular momentum addition rules would yield the symmetry of the resulting electron-hole pair states to be those of the spherical harmonics L and M with $L = 1, 2, 3$ and $-L \le M \le L$. Indeed, the pair states have a three-dimensional representation T_{1P} corresponding to $L = 1$ and a five-dimensional representation H_P corresponding to $L = 2$. However, since C_{60} does not have complete spherical symmetry, the $L = 3$ states split into two groups, a three-dimensional representation T_{2P} and a four-dimensional one G_P. The symmetry-adapted electron-hole pair spin-singlet states may be written as linear combinations

$$\big|LNp_ep_h\big\rangle = \sum_{m_e=-1}^{1}\sum_{m_h=-2}^{2} C^{12}_{m_em_h}(LN)c^{+}_{1p_em_e}c_{2p_hm_h}|0>, \tag{3.3}$$

where the operator c^{+}_{lpm} (c_{lpm}) creates (annihilates) an electron in a molecule state $|lpm>$ with a single-particle parity p. The coefficients on the right of Eq. (3.3) are related to the Clebsch-Gordan coefficients $C^{LM}_{lml'm'}$[27] by ($L = 1, 2$ with $-L \le N \le L$ and $L = 3$ with $N = 0, \pm1$)

$$\begin{aligned}
C^{12}_{m_em_h}(LN) &= (-1)^{-m_h}C^{LN}_{1m_e2-m_h},\\
C^{12}_{m_em_h}(3,\pm3) &= (-1)^{-m_h}\left[\sqrt{\frac{2}{5}}C^{3\pm3}_{1m_e2-m_h}\right.\\
&\qquad\left.\pm\sqrt{\frac{3}{5}}C^{3\mp2}_{1m_e2-m_h}\right],\\
C^{12}_{m_em_h}(3,\pm2) &= (-1)^{-m_h}\left[\sqrt{\frac{2}{5}}C^{3\mp2}_{1m_e2-m_h}\right.\\
&\qquad\left.\mp\sqrt{\frac{3}{5}}C^{3\pm3}_{1m_e2-m_h}\right].
\end{aligned} \tag{3.4}$$

The symmetry-adapted pair states are chosen such that quantum numbers L and N, with $L = 1$ corresponds to the basis of the irreducible representation T_{1P}, $L = 2$ to H_P, $L = 3$ and $N = 0, \pm3$ to T_{2P} and $L = 3$ and $N = \pm1, \pm2$ to G_P.

The true singlet exciton states are linear combinations of the symmetry-adapted pair states (3.3)

$$\big|LNP\Lambda\big\rangle = \sum_{p=+,-} c_{\Lambda p}(LNP)\,\big|LNP{\cdot}p\ p\big\rangle, \tag{3.5}$$

where the summation runs over the hole parity p. The summation in Eq. (3.5) indicates that pair states of different single-particle parities may be coupled provided that the total parity P is conserved. The fourth quantum number Λ labels the two coupled pair states of the same symmetry. The four quantum numbers, L, N, P, and Λ span the 60 pair states (without spin) under consideration. The eigenstates (3.5) of the Frenkel excitons are orthonormalized with $\sum_p c^{*}_{\Lambda p}c_{\Lambda' p} = \delta_{\Lambda\Lambda'}$, following the orthonormalization property of the Clebsch-Gordan coefficients.

The symmetry-adapted basis pair states $|LNP{\cdot}p\ p>$ of Eq. (3.3) with the third quantum number set to $p_e = P{\cdot}p$ block-diagonalize the two-body Hamiltonian of the π-electron system including the full Coulomb interaction v into 2×2 matrices diagonal in the quantum numbers L, N, and P:

$$\begin{aligned}
&\big\langle LNP{\cdot}p\ p\big|H\big|L'N'P'{\cdot}p'\ p'\big\rangle\\
&= \delta_{LL'}\delta_{NN'}\delta_{PP'}\left\{\delta_{pp'}\left[\varepsilon_{1P\cdot p}-\varepsilon_{2p}\right]\right.\\
&\quad\left.+\big\langle LNP{\cdot}p\ p\big|v\big|LNP{\cdot}p'\ p'\big\rangle\right\},
\end{aligned} \tag{3.6}$$

with the electron in the level with the excitation energy ε_{1p_e} and the hole in the level with ε_{2p_h} and with the Coulomb interaction connecting pair states with (p_e, p_h) and $(-p_e, -p_h)$. In our notation system, the exciton energy eigenvalues $E_{LNP\Lambda}$ are independent of N for $L = 1, 2$, i.e. $(2L+1)$-fold degenerate. For $L = 3$, the exciton energies for the two symmetry sets of $N = 0, \pm3$ and of $N = \pm1, \pm2$ are different but degenerate within each set.

B. Coulomb interaction

The Coulomb interaction term in Eq. (3.6) includes the electron-hole attraction, and the exchange term to the electron-hole attraction[24] with the diagrammatic representation in Fig. 3. The exchange terms of Fig. 3b only exist for the spin-singlet exciton. Assuming non-overlap of the p_z-orbitals from different carbon sites of the π-like molecule states, we express the Coulomb term in Eq. (3.6) in terms of the single-particle eigenstates of Eqs. (2.2) and (2.8) as

$$\begin{aligned}
&\big\langle LNp_ep_h\big|v\big|LNp'_ep'_h\big\rangle =\\
&-\frac{15}{(60)^2}\sum_{g,g'}G^{*}_{LN}(12p_ep_h|\mathbf{gg'})v(\mathbf{g}-\mathbf{g'})G_{LN}(12p'_ep'_h|\mathbf{gg'})\\
&+2\frac{15}{(60)^2}\sum_{g,g'}G^{*}_{LN}(12p_ep_h|\mathbf{gg})v(\mathbf{g}-\mathbf{g'})G_{LN}(12p'_ep'_h|\mathbf{g'g'})
\end{aligned} \tag{3.7}$$

with

$$\begin{aligned}
&G_{LN}(l_el_hp_ep_h|\mathbf{gg'}) =\\
&\sum_{m_e=-l_e}^{+l_e}\sum_{m_h=-l_h}^{+l_h} C^{l_el_h}_{m_em_h}(LN)e^{*}_{l_ep_em_e}(\mathbf{g})e_{l_hp_hm_h}(\mathbf{g'}),
\end{aligned} \tag{3.8}$$

where the coefficients $C^{l_el_h}_{m_em_h}(LN)$ are defined in Eq. (3.4). The Coulomb potential takes the form

$$v(\mathbf{g}) = U\delta_{g0} + \frac{e^2}{\epsilon R_0}\frac{1}{|\mathbf{g}|}(1-\delta_{g0}), \tag{3.9}$$

where U denotes the one-site Coulomb matrix element of the p_z orbitals. R_0 is the distance from a carbon atom to the center of the cage and ϵ denotes a dielectric constant representing the screening of the interatomic (but intramolecule) Coulomb interaction.

The first term on the right of Eq. (3.7) comes from the direct electron-hole attraction and the second is the exchange counter part. The factor of 2 may be viewed as originating from the spin degeneracy or the structure of the singlet. The double sums over the carbon sites in expression (3.7) may be reduced to single sums, by means of the product relation for the Wigner D-functions representing the two rigid-body transformations to the sites. Thus, with a simplifying definition for the Coulomb matrix element:

$$V_{pp'}(LNP) \equiv -\langle LNP{\cdot}p\ p|v|LNP{\cdot}p'\ p'\rangle \tag{3.10}$$
$$= -\frac{U}{60}F_{pp'}(LNP) + \frac{e^2}{\epsilon R_0}\left[H_{pp'}(LNP) - 2X_{pp'}(LNP)\right],$$

which the $N-$dependence serves only to differentiate between T_{2P} and G_P in the $L = 3$ case. For $L = 1, 2$ ($-L \le N \le L$) and $L = 3$ ($N = 0, \pm 1$), the intraatomic Coulomb interaction is given by

$$F_{pp'}(LNP) = \tag{3.11}$$
$$\frac{15}{2L+1}\sum_{M=-L}^{+L} G^*_{LM}(12P{\cdot}p\ p|\mathbf{ee})G_{LM}(12P{\cdot}p'\ p'|\mathbf{ee})$$

and the interatomic Hartree and exchange contributions

$$H_{pp'}(LNP) = \frac{1}{4(2L+1)}\sum_{M=-L}^{+L}{\sum_g}' \tag{3.12}$$
$$G^*_{LM}(12P{\cdot}p\ p|\mathbf{ge})\frac{1}{|\mathbf{g}-\mathbf{e}|}G_{LM}(12P{\cdot}p'\ p'|\mathbf{ge}),$$

$$X_{pp'}(LNP) = \frac{1}{4(2L+1)}\sum_{M=-L}^{+L}{\sum_g}' \tag{3.13}$$
$$G^*_{LM}(12P{\cdot}p\ p|\mathbf{gg})\frac{1}{|\mathbf{g}-\mathbf{e}|}G_{LM}(12P{\cdot}p'\ p'|\mathbf{ee}),$$

where the functions G_{LM} are defined in Eq. (3.8). The intraatomic term, Eq. (3.11), includes both the Hartree and exchange contributions.

In Table I are listed the values of these three terms evaluated from Eqs. (3.11–3.13). The corresponding results using the continuum approximation of Ref. 8 differ little for the Hartree contributions, but up to 50 % for the exchange terms. Table I indicates that the interatomic electron-hole exchange may be neglected in comparison with the interatomic electron-hole attraction. This is in complete contrast to the intraatomic case, which is exchange-dominated since the singlet exciton has twice the number of exchange terms of equal magnitude as the direct attraction (cf. Fig. 3). Since the prefactor $U/60$ is smaller than $e^2/(\epsilon R_0)$, it is evident that the diagonal elements, $V_{pp}(LNP)$, in Eq. (3.10) are dominated by the interatomic Hartree matrix elements, and are, therefore, positive. The off-diagonal elements $p \neq p'$ are strongly influenced by the intraatomic exchange. They are often negative (except for T_{1G} and H_U). Table I also shows that a contact-potential approximation, where the interatomic Coulomb interactions are neglected, is invalid.

C. Pair excitation energies and ground-state stability

With the Coulomb interaction given in Table I, the 2×2 eigenvalue problems for the 60 Frenkel excitons originated from the closest π-electron-related HOMO and LUMO single-particle states can be solved. For a given representation T_1, H, T_2, or G and a given total parity $P = \pm 1$, the 2×2 Hamiltonian for hole states of parities p and p' may be written as

$$H_{pp'} = (\bar{E} + p\Delta)\delta_{pp'} - \tilde{U}(1 - \delta_{pp'}), \tag{3.14}$$

where

$$\bar{E} = \frac{1}{2}(E_+ + E_-),$$
$$\Delta = \frac{1}{2}(E_+ - E_-),$$
$$\tilde{U} = V_{+-}(LNP),$$
$$E_p = \varepsilon_{1P\cdot p} - \varepsilon_{2p} - V_{pp}(LNP). \tag{3.15}$$

The two exciton eigenvalues $E_{LNP\Lambda}$ with $\Lambda = \pm 1$ and the corresponding eigenvectors follow as

$$E_{LNP\Lambda} = \bar{E} + \Lambda\sqrt{\Delta^2 + \tilde{U}^2},$$
$$c_{\Lambda P}(LNP) = \delta_{\Lambda\cdot p,+}\cos\eta + \delta_{\Lambda\cdot p,-}\, p\cdot\sin\eta, \tag{3.16}$$

where

$$\sin(2\eta) = \tilde{U}/\sqrt{\Delta^2 + \tilde{U}^2}. \tag{3.17}$$

The coupling of the Frenkel excitons with the same representation and parity P destroys the simple picture that the reduction of the difference of the single-particle energies $\varepsilon_{1P\cdot p} - \varepsilon_{2p}$ in Eq. (3.15) by V_{pp} defines the binding energy of the exciton. The ratio $\tilde{U}/\sqrt{\Delta^2 + \tilde{U}^2}$ determines the strength of the redistribution of the two coupled excitons with $\Lambda = \pm 1$. Therefore, the sign of $\tilde{U}$ plays an important role for the actual oscillator strength for the excitations of electron-hole pairs with different Λ as will be discussed in Sec. IV B.

In Figs. 4 and 5 a selected set of pair excitation energies are plotted versus the strength of the interatomic Coulomb interaction $e^2/(\epsilon R_0)$ for two different values of the intrasite Coulomb matrix element U. To avoid clutter in Fig. 4, only plotted are excitons of representations T_{1P} ($L = 1$) and H_P ($L = 2$), i.e., a total of eight exciton energies with $P = \pm 1$ and $\Lambda = \pm 1$. The other eight exciton energies for the representations T_{2P} and G_P ($L = 3$)

are not plotted since they do not usually appear in the optical spectra considered below. Figure 5 compares the four lowest pair excitations T_{1G}, T_{2G}, G_G, and H_G with the A_G Hartree-Fock ground state with even parity. The two intraatomic interaction values chosen are $U = 0$ and $U = 4V$. The Coulomb energy U when two electrons are in the same atomic p-orbital is usually estimated to be $U \approx 10$–20 eV. If one uses a hydrogenlike wave function with an effective nuclear charge $z_{eff} = 3.25$, a value of $U = 17.3$ eV results[8]. With reasonable values for the hopping parameter V (cf. Sec. II), $U = 4V$ is close to the estimated values. Both Figs. 4 and 5 show that the explicitly chosen U value has a minor influence on the excitation energies. A strong intraatomic Coulomb interaction $U = 4V$ shifts the pair energies slightly to higher energies by about $0.05V$.

The dependence on the variation of the interatomic Coulomb interaction $e^2/(\epsilon R_0)$ is explored because of the uncertainty of the value for the dielectric constant used to screen the interatomic interaction. The range goes from the limit of metallic screening ($\epsilon = \infty$) to the limit of the unscreened Coulomb interaction, ($\epsilon = 1$). With $R_0 \approx 3.5\mathring{A}$ and the range of the hopping parameter V in Sec. II, the maximum value of $e^2/(\epsilon R_0 V)$ is about 1.1. In the literature, screening values between 3 and 10 have been reported. For instance, dielectric constants for solid fullerites have been determined as $\epsilon = 3.5$, 3.9, or 4.4[32–34]. A dielectric constant in a model cluster of 7.13 to 9.86 has been used in Ref. 35 to study the van-der-Waals cohesion energy. Other authors[36] use $\epsilon = 4.4$ and 6.5 to explain the screening in C_{60} clusters. Hansen et al.[37] reported a value $\epsilon = 4.6$ derived from a Kramers-Kronig analysis of their visible-UV EELS spectrum. For $\epsilon = 4.6$, the interaction parameters of $e^2/(\epsilon R_0 V) \approx 0.19$ (0.23, 0.14) result from $V = 4.626$ (3.83, 6.61) eV. From Fig. 4, evidently the interatomic Coulomb interaction has much more influence on the pair-excitation energies than the onsite Coulomb interaction. Moreover, its presence gives rise to an effective attractive interaction between electrons and holes. The exciton binding noticeably reduces the pair excitation energies. Typical reductions amount to about $0.8e^2/\epsilon R_0$ for T_{1G}, H_G, H_U, and G_G and vanishing intraatomic interaction U. For T_{1U} (T_{2G}), slightly smaller (larger) values of 0.5 (1.0) $e^2/\epsilon R_0$ are shown in Figs. 4 and 5. The reductions corresponding to finite U values are smaller.

The drastic reduction of the electron-hole pair excitation energies by the interatomic Coulomb interaction is illustrated in Fig. 5 for the lowest excitations with even parity. The figure indicates that for sufficiently weak screening, pair energies may even become negative. For T_{2G} this happens if $\epsilon < 6.5$ eV$/V$ (when $U = 0$) or $\epsilon < 5.5$ eV$/V$ (when $U = 4V$). For $V = 3.83$ this corresponds to $\epsilon < 1.7$ or $\epsilon < 1.4$. For a very strong (i.e. almost unscreened) interatomic Coulomb interaction, the lowest T_{2G} pair excitation replaces the closed-shell Hartree-Fock state A_G as the ground state of the C_{60} molecule. This transition should be accompanied by a spontaneous symmetry breaking to lift the degeneracy of the lower T_{2G} states with respect to the quantum number N.

The findings in Figs. 4 and 5 are consistent with the results of quantum-chemical calculations[10–12]. The energies of the $^1T_{1G}$, $^1T_{2G}$, and ^1G_G multiplets are quasi-degenerate, within a range of 0.1 eV, at about 0.5 eV and the ^1H_G multiplet is higher, separated by about 0.4 eV. Figure 5 (b) ($U = 4V$) indicates a similar situation for reasonable parameters of $e^2/(\epsilon R_0 V) \approx 0.2$–$0.5$ discussed above.

The comparison with the quantum-chemical results may be used to fix our model parameters. In the unscreened case $\epsilon = 1$ the disagreement is too large. When the effect of the interatomic Coulomb interaction is somewhat screened, e.g. in the case of $U = 17.3$ eV and an intermediate effective screening of $\epsilon = 4.6$, the agreement is improved. For the three hopping parameters $V = 4.626$ (3.83, 6.61) eV we find 2.86 (2.53, 3.90) eV for T_{1G}, 3.06 (2.65, 4.24) eV for T_{2G}, and 2.75 (2.46, 3.71) eV for G_G, and 3.16 (2.71, 4.41) eV for H_G. Consequently, we conclude that the effective interatomic Coulomb interaction has to be effectively screened. For the hopping parameter $V = 3.83$ eV, $\epsilon = 4.6$ is the appropriate value. For the larger hopping parameter $V = 4.626$ eV the screening has to be slightly increased. The largest hopping parameter $V = 6.61$ eV should be excluded since the dielectric constant becomes unreasonably large. The resulting picture is also more or less consistent with quasiparticle calculations for solid C_{60}[14] which yield the lowest excitation energy of 2.15 eV for the $h_u \rightarrow t_{1u}$ transition. When the electron-hole interaction is included[38] this value is reduced to 1.57 eV giving an exciton binding energy of 0.58 eV. This *ab initio* band calculation also gives peak positions for T_{2G}, T_{1G}, G_G, and H_G that are redshifted in comparison to the peak positions 1.86, 1.94, 2.03, and 2.30 eV in the fine structure of the forbidden absorption edge of the fullerite[38]. An inconsistency among the first-principles calculations is the energy ordering of the T_{1G} and T_{2G} excitations. In Refs. 10,11 the symmetry of the lowest excitation is T_{1G} whereas other calculations[12,38] indicate the T_{2G} level to be the lowest one. Figure 5 shows that the answer depends on the relative strengths of the intra- and interatomic Coulomb interactions. For $U = 0$, T_{2G} represents the lowest excited state. For $U = 4V$, this holds only for $e^2/(\epsilon R_0 V) \geq 0.7$. In the more interesting region of lower interatomic values T_{1G} is favored. For even smaller values of interatomic interaction, G_G becomes the ground state.

IV. OPTICAL SPECTRA

A. Optical transitions

The coupling of light to the π-electron system of the C_{60} molecule is governed by the polarization operator

$$\hat{P}_\alpha = \sum_{\nu,\nu'} \langle \nu \left| e x_\alpha \right| \nu' \rangle \, c_\nu^+ c_{\nu'} \,, \tag{4.1}$$

where x_α is the α-th Cartesian component of the position operator. With the restriction to the LUMO and HOMO states described in Sec. II and a strong localization of the p_z orbitals as in the case of the description of the Coulomb interaction in Eq. (3.9), the dipole matrix elements take the form ($\nu \equiv lpm$):

$$\langle lpm \left| e x_\alpha \right| l'p'm' \rangle = eR_0 \frac{\sqrt{(2l+1)(2l'+1)}}{60} \sum_g e^*_{lpm}(\mathbf{g}) \mathrm{g}_\alpha e_{l'p'm'}(\mathbf{g}). \tag{4.2}$$

The sum over the carbon positions can be evaluated using the symmetry properties[27]:

$$\langle lpm \left| e x_\alpha \right| l'p'm' \rangle = \delta_{p,-p'} D(ll'|pp') \sum_{M=-1}^{+1} (-1)^{m'} C^{1M}_{lml'-m'} A^1_{\alpha M}, \tag{4.3}$$

where the effective dipole moment is given by

$$D(ll'|pp') = eR_0 \frac{\sqrt{(2l+1)(2l'+1)}}{3} \times \left[-\sqrt{2} G_{11}(ll'pp'|\mathbf{ee})\mathrm{e}_x + G_{10}(ll'pp'|\mathbf{ee})\mathrm{e}_z \right], \tag{4.4}$$

with $G_{LN}(ll'pp'|\mathbf{ee})$ defined in Eq. (3.8) for the reference atom at position $\mathbf{e}$, and the projection of the Cartesian components onto the $L = 1$ angular momentum states,

$$A^1_{\alpha M} = \delta_{\alpha x} \frac{1}{\sqrt{2}} (\delta_{M-1} - \delta_{M1}) + \delta_{\alpha y} \frac{i}{\sqrt{2}} (\delta_{M1} + \delta_{M-1}) + \delta_{\alpha z} \delta_{M0}. \tag{4.5}$$

The optical transition matrix elements from the A_G ground state to the electron-hole pair excited states introduced in Eq. (3.3) are

$$\left\langle LNp_e p_h \left| \hat{P}_\alpha \right| 0 \right\rangle = \delta_{L1} \delta_{p_e,-p_h} D(12|p_e p_h) A^1_{\alpha N} \,. \tag{4.6}$$

Selection rules limit excitations to $L = 1$ excitons with odd parity, i.e. T_{1U} states[10,12]. Out of the 60 singlet excitons there are only six such states, namely $|1N + - >$ and $|1N - + >$ with $N = -1, 0, 1$. Because of the different structures of the single-particle eigenvectors in Eq. (2.8) the oscillator strengths vary with the parity-allowed pairs:

$$D(12|+-) = -0.48547 eR_0 \quad D(12|-+) = -0.55626 eR_0. \tag{4.7}$$

The characteristic dipole length is about half the distance from a carbon atom to the center of the cage.

The coupling of two different excitonic states by an external electric field via the polarization operator is

$$\left\langle LNp_e p_h \left| \hat{P}_\alpha \right| L'N'p'_e p'_h \right\rangle = \sum_{m_e, m'_e=-1}^{+1} \sum_{m_h, m'_h=-2}^{+2} (-1)^{-m_h - m_{h'}} C^{LN}_{1m_e 2-m_h} C^{L'N'}_{1m'_e 2-m'_h} \times \{ -\delta_{p_e p'_e} \delta_{m_e m'_e} \langle 2p'_h m'_h \left| e x_\alpha \right| 2p_h m_h \rangle + \delta_{p_h p'_h} \delta_{m_h m_{h'}} \langle 1p_e m_e \left| e x_\alpha \right| 1p'_e m'_e \rangle \}. \tag{4.8}$$

We record here a special case needed later for the nonlinear optical spectra, by Eq. (4.3),

$$\left\langle 2Npp \left| \hat{P}_\alpha \right| 1N' {-p'}\ p' \right\rangle = \sqrt{\frac{3}{20}} \left[\delta_{pp'} \sqrt{5} D(11|p\ {-p}) + \delta_{p,-p'} D(22|{-p}\ p) \right] \times (-1)^{N'} \sum_{M''=-1}^{+1} C^{1M}_{2N1-N'} A^1_{\alpha M}, \tag{4.9}$$

with $D(11|-+) = D(11|+-) = -0.70700 eR_0$ and $D(22|+-) = D(22|-+) = 0.75585 eR_0$. The dipole-allowed transitions from T_{1U} to both H_G and T_{1G} excitons are possible because of the difference of the C_{60} symmetry group from the spherical symmetry.

B. Linear absorption: Optically allowed excitons

Consider first the case of the A_G ground state. Its optical properties are governed by the time-dependent polarization field

$$P_\alpha(t) = 2n \left\langle 0 \left| \hat{P}_\alpha(t) \right| 0 \right\rangle, \tag{4.10}$$

where n is the density of the buckyballs. The linear response in the rotating-wave approximation is, following Eq. (4.6), given by

$$\chi^{(1)}_{\alpha\beta}(\omega) = \delta_{\alpha\beta} 2n \sum_{\Lambda=+,-} \frac{\left| \sum_{p=+,-} c_{\Lambda p}(1-) D(12|{-p}\ p) \right|^2}{E_{1-\Lambda} - \hbar\omega - i\Gamma_{1-\Lambda}}, \tag{4.11}$$

where ω is the frequency of light and a phenomenological lifetime-broadening parameter $\Gamma_{LP\Lambda}$ has been introduced for the electron-hole pair states. The diagonality and isotropy of the susceptibility tensor follows immediately from $\sum_{M=-1}^{+1} A^{1^*}_{\alpha M} A^1_{\beta M} = \delta_{\alpha\beta}$.

The resulting low-energy absorption spectrum of the π-electron system is shown in Fig. 6 for various values of the effective intraatomic Coulomb interaction U. The ratio of the interatomic and intraatomic Coulomb interaction has been fixed at the values $e^2/(\epsilon R_0 U) = 0.2377$ (left panel) and 0.0517 (right panel). Using an intrasite matrix element $U = 17.3$ eV the two values correspond to the cases of no screening of the interatomic interaction ($\epsilon = 1$) and of intermediate screening ($\epsilon = 4.6$). In

the spectral range considered the absorption in the π-electron system exhibits two T_{1U} exciton peaks at about $E_{1--} \approx V + 0.012U - 0.666\frac{e^2}{\epsilon R_0}$ and $E_{1-+} \approx 1.139V + 0.039U - 0.488\frac{e^2}{\epsilon R_0}$ with different oscillator strengths.

Comparison of the calculated absorption spectrum with experiment leads to a discussion of two salient points: (i) the comparison of the calculated and measured peak positions and (ii) the relative intensities of the two absorption peaks. The two calculated exciton peaks should be compared to the measured absorption peaks at 3.81 and 4.90 eV[39], or 3.65 and 4.72 eV[40], or 3.78 and 4.84 eV[41]. The weak structure observed at lower energies, in particular the weak peak at 2.73 eV, for solid C_{60}[40] has been ascribed to dipole-forbidden transitions, which become partially allowed due to lattice fluctuations, interface effects and/or internal electric fields. The same holds for the small structure occurring in the energy region of 2 eV in spectra of C_{60} isolated in a noble gas matrix[39]. The intense absorption band close to 5.96 eV[40] or 5.87 eV[41] only possesses a partial π character and is also beyond the scope of our study. The identification of the lower and upper T_{1U} excitons ($L = 1$, $P = -$) with the two absorption peaks under consideration restricts the range for the values of the parameters U and $e^2/(\epsilon R_0)$. If we take the strong onsite interaction value $U = 17.3$ eV, the dielectric constant varies drastically between $\epsilon \approx 2$ (for the hopping parameter $V = 4.62$ eV) and $\epsilon \approx 10$ (for $V = 3.83$ eV). With a weaker $U \approx 10$ eV, the range of the dielectric constant is reduced to $2.5 < \epsilon < 4.8$.

The theoretical result that the absorption peak at lower energy possesses a smaller oscillator strength than the peak at higher energy is in agreement with the experimental observation. Within the single-particle approximation, i.e., for $U = 0$ and $e^2/(\epsilon R_0) = 0$, the oscillator strengths of the two transitions $h_u \to t_{1g}$ and $h_g \to t_{1u}$ between molecule levels are similar, from Eq. (4.7). The reduction of the ratio of the oscillator strength of the lower-energy peak to that of the higher-energy peak may be understood in terms of the Coulomb coupling of the two T_{1U} excitons, as is evident from the presence of the eigenvectors $c_{\Lambda p}(1-)$ from Eq. (3.16) in the oscillator strength of Eq. (4.11). Since the dipole matrix elements $D(12|+-)$ and $D(12|-+)$ have the same sign and nearly equal magnitudes, the oscillator strengths of the two T_{1U} excitations are governed by the relative sign of the coefficients $c_{\Lambda p}(1-)$, and so by the sign of the coupling term $V_{+-}(1-)$ in Eq. (3.10). The domination of the exchange term leads to $V_{+-}(1-) < 0$ and, hence, the oscillator strength of the low-energy exciton at $\hbar\omega = E_{1--}$ is reduced compared to the high-energy absorption at $\hbar\omega = E_{1-+}$. This shows not only that the relative strengths of the two exciton peaks are influenced by the Coulomb interaction but also that the intersite interaction is indispensable.

Let us consider briefly the consequences on the linear optical spectra of the fascinating possibility raised in Sec. III that the excitonic state T_{2G} is the ground state rather than the closed-shell A_G state. In the energy region of the two allowed single-particle transitions $h_u \to t_{1g}$ and $h_g \to t_{1u}$, two peaks can arise from the transitions between the lowest T_{2G} state to the two H_U and two G_U states (see Fig. 4) satisfying both the angular momentum and parity selection rules. Their oscillator strengths are governed by the moments $D(11|+-)$ and $D(22|-+)$. The transition energies may also be accounted for by the parameter values for V, U, and $e^2/(\epsilon R_0)$ already discussed in connection with Fig 5. However, the single-particle energies from the new excitonic ground state have to be recalculated and compared with the measurements by photoemission and inverse photoemission. Since in the exciton ground state there is already one electron in a LUMO and a hole in a HOMO state, the one-particle excited state has strong correlation effects. The interaction effects can split the degeneracies of the HOMOs and the LUMOs, leading to more than two electron and two hole single-particle states. The group-theoretical indentities $t_{1p} \times T_{2G} = g_p + h_p$ and $h_p \times T_{2G} = t_{1p} + t_{2p} + g_p + h_p$ ($p = g, u$) give us a rough idea of the single-particle multiplets. The symmetry breaking which will remove the degeneracy of the T_{2G} states would reduce the number of one-particle excited states.

C. Electro-optic Kerr effect: Electric-field-induced forbidden excitons

In the theoretical linear optical spectra, the parity selection rule excludes the same-parity transitions, such as those lowest in energy, $h_u \to t_{1u}$. They can, however, be induced by the application of a static electric field which mixes the even-parity excitons with the odd-parity excitons. The linear response to the external laser field of the electric polarization, Eq. (4.10), to second order in an applied static electric field $\mathbf{F}$ (the Kerr effect), is closely related to the third-order susceptibility, to be derived in Sec. IV D. By a similar derivation leading to Eq. (4.15), the static electric field effect on the linear optical response is given by

$$\chi^{(1)}_{\alpha\beta}(\omega) = 2nP_{\alpha\beta}(\hat{F})\frac{F^2}{4}\sum_{L=1}^{2}\sum_{\Lambda',\Lambda''=\pm}\frac{S^*_{L\Lambda'}S_{L\Lambda''}}{(E_{1-\Lambda'} - E_{L+-})(E_{L+-} - \hbar\omega - i\Gamma_{L+-})(E_{1-\Lambda''} - E_{L+-})}, \tag{4.12}$$

with the prefactor depending on the direction of the applied static field denoted by its unit vector $\hat{F}$ relative to the light polarization direction:

$$P_{\alpha\beta}(\hat{F}) = \frac{3}{10}(3\delta_{\alpha\beta} + \hat{F}_\alpha\hat{F}_\beta), \tag{4.13}$$

and the oscillator strength $S_{L\Lambda}$ given in Eq. (4.17).

The selection rules $\Delta L = 0, \pm 1$ confine the contributions to the Kerr effect from the H_G and T_{1G} excitons. Because of the random orientations of the C_{60} molecules

in solutions or in the face-centered cubic thin films[42–44], the dependence of the field direction of the prefactor is in practice averaged out to $P_{\alpha\beta}(\hat{F}) = \delta_{\alpha\beta}$. Only in the case of the low-temperature simple cubic crystals of undoped C_{60} is there a chance of experimentally partially probing the polarization dependence. The four molecules per unit cell are rotated by an angle ϕ around a space diagonal axis [111], [1$\bar{1}\bar{1}$], [$\bar{1}$1$\bar{1}$], or [$\bar{1}\bar{1}$1]. The angle of rotation is found to be $\phi = 22 - 26^{\circ}$[42–44].

The spectrum of the electrooptic Kerr effect is presented in Fig. 7 as a function of the reduced photon energy for different model parameters of the effective Coulomb interaction, U and $e^2/\epsilon R_0$. The electric field strength has been fixed at $eFR_0/(2V) = 0.001$ to compare with the allowed transitions in zero field in Fig. 6, corresponding to 2.6×10^5 V/cm for a hopping parameter of $V = 4.626$ eV. The positions of the field-induced excitons are approximately given by $E_{2+-} = 0.757V + 0.019U - 0.760e^2/\epsilon R_0$ for the H_G exciton or $E_{1+-} = 0.757V + 0.0121U - 0.986e^2/\epsilon R_0$ for the T_{1G} exciton. Their energy difference is determined by the interatomic Coulomb interaction, $E_{2+-} - E_{1+-} \approx 0.226e^2/\epsilon R_0 \approx 0.93$ eV$/\epsilon$. For intermediate screening, it is smaller than the line broadening used in Fig. 7, explaining the appearance of only one pronounced field-induced peak in the absorption spectrum below the energy of the lower allowed T_{1U} exciton (in Fig. 4). Only for very weak screening does a weak second T_{1G}-related peak appear at an energy below the more intense H_G-related peak (see the solid and dashed curves in Fig. 7a).

These general findings seem to be in agreement with the results inferred from different nonlinear optical experiments, such as two-photon absorption[45] and degenerate four wave mixing[46]. A two-photon resonance at 2.73 eV or 2.67 eV is observed and identified with an H_G exciton. Such energy values are within the range of the theoretical values given by the parameters under discussion. The prediction of a field-induced H_G exciton line also explains the weak absorption structure around 2.73 eV[40]. The theoretical energy ordering $T_{1G} < H_G < T_{1U}$ clearly visible in Figs. 4 and 5 agrees with results of the second-harmonic generation (SHG) on a surface[47,48], where a resonance near 1.8–1.9 eV is identified with a T_{1G} exciton. However, the theoretical prediction of the energy splitting between T_{1G} and H_G is smaller than the experimental value of 0.8–0.9 eV if we choose our model parameters, such as $U = 17.3$ eV, $\epsilon = 4.6$, to obtain similar exciton energies as the quantum-chemical calculations.

D. Third-harmonic generation

In this section, we consider another nonlinear optical experiment, the third-harmonic generation (THG). A three-photon resonance occurs when three times the fundamental photon energy is equal to the lowest $A_G \rightarrow T_{1U}$ one-photon dipole-allowed transition (in the single-particle picture: $h_u \rightarrow t_{1g}$ and $h_g \rightarrow t_{1u}$). From the general expression for the third-order susceptibility given by Armstrong et al.[49], we take into account only triply resonant contributions to the susceptibility describing THG. Neglecting biexciton effects[50] and using the dipole matrix elements (4.6) and (4.9) we find

$$\chi^{(3)}_{\alpha\beta\gamma\delta}(\omega) = \frac{2n}{3!}\mathrm{P}_{\beta\gamma\delta}\sum_{L=1}^{2}\sum_{N=-L}^{+L}\sum_{N',N''=-1}^{+1}\sum_{\Lambda,\Lambda',\Lambda''=\pm1} \left\langle 0\left|\hat{P}_\alpha\right|1N'-\Lambda'\right\rangle \frac{\left\langle 1N'-\Lambda'\left|\hat{P}_\beta\right|LN+\Lambda\right\rangle}{(E_{1-\Lambda'}-3\hbar\omega-i\Gamma_{1-\Lambda'})} \frac{\left\langle LN+\Lambda\left|\hat{P}_\gamma\right|1N''-\Lambda''\right\rangle}{(E_{L+\Lambda}-2\hbar\omega-i\Gamma_{L+\Lambda})} \frac{\left\langle 1N''-\Lambda''\left|\hat{P}_\delta\right|0\right\rangle}{(E_{1-\Lambda''}-\hbar\omega-i\Gamma_{1-\Lambda''})}. \quad (4.14)$$

Here, n is the density [cf. Eq. (4.10)] and $\mathrm{P}_{\beta\gamma\delta}$ denotes the sum over all permutations of β, γ, and δ ensuring that the fourth-rank tensor third-order susceptibility is independent of the ordering of those three indices, i.e., the Cartesian components of the three fields creating the third-order harmonic.

Selection rules dictate that the three-photon resonance takes the system from the A_G ground state to the $L = 1$ excitons with odd parity (T_{1U}), and from T_{1U} to $L = 2$ (H_G) and $L = 1$ (T_{1G}) excitons with even parity, which may give rise to the doubly resonant terms. We restrict ourselves to the double-resonance terms with the lower-energy ($\Lambda = -$) excitons. The higher-lying excitons are energetically well separated from the frequency region of interest (cf. Fig. 4). Consequently the $|LN+-\rangle$ states may be approximately replaced by the uncoupled $|LNpp\rangle$ ($p = +$, $L = 1, 2$) states, corresponding to the single-particle transitions $h_u \rightarrow t_{1u}$. The third-order susceptibility becomes

$$\chi^{(3)}_{\alpha\beta\gamma\delta}(\omega) = 2nG_{\alpha\beta\gamma\delta}\sum_{L=1}^{2}\sum_{\Lambda',\Lambda''=\pm} \frac{S^*_{L\Lambda'}}{(E_{1-\Lambda'}-3\hbar\omega-i\Gamma_{1-\Lambda'})} \frac{S_{L\Lambda''}}{(E_{L+-}-2\hbar\omega-i\Gamma_{L+-})\,(E_{1-\Lambda''}-\hbar\omega-i\Gamma_{1-\Lambda''})}, \quad (4.15)$$

with the polarization-dependent prefactor

$$G_{\alpha\beta\gamma\delta} = \frac{1}{8}\mathrm{P}_{\beta\gamma\delta}\sum_{M=-2}^{+2} F^*_{\alpha\beta}(M)F_{\delta\gamma}(M), \quad (4.16)$$

$$F_{\alpha\beta}(M) = \sum_{M',M'=-1}^{+1}(-1)^{M'}A^1_{\alpha M'}C^{1M''}_{2M1-M'}A^1_{\beta M''},$$

and the oscillator strength

$$S_{L\Lambda} = \sum_{p=\pm} c^*_{\Lambda p}(1-)D(12|-p\;p)$$

$$\times \left[\frac{1}{\sqrt{5-2L}} c_{\Lambda+}(1-) D(11|+-) \right.$$
$$\left. + \sqrt{\frac{5-2L}{5}} c_{\Lambda-}(1-) D(22|-+) \right]. \qquad (4.17)$$

Eq. (4.15) may be interpreted as the third-order susceptibility of a five-level system: ground state A_G, even-parity excited states H_G or T_{1G}, and the two odd-parity excited states T_{1U}, in contrast to the third-order susceptibility of a three-level system used to fit the experimental measurements[51,52]. Moreover, the symmetry of the states participating in the THG process are well defined here. On the other hand, only the most dominant resonant terms are considered here, whereas the formulas used to fit the data also include less important resonant and nonresonant terms.

The spectral behavior of the magnitude of the third-order susceptibility is plotted in Fig. 8 for the same set of model parameters as in Fig. 7. Only the lower T_{1U} excitons appear. Despite the presence of many exciton levels, in the spectral region considered only a pronounced double-peak structure or one broad peak appears. In the case of stronger screening of the intersite Coulomb interaction (the right panel of Fig. 8), the high-energy peak corresponds to the two-photon resonance with the $L = 2$, $P = +$ (H_G) exciton. It is enhanced by the resonance with the T_{1G} excitons ($L = 1$, $P = +$). The three-photon resonance at the frequency of the fundamental light wave occurs at slightly lower energies defined by the electric-dipole-allowed $L = 1$, $P = -$ (T_{1U}) exciton. On the other hand, in the case of the weaker screening (the left panel), for the curves going from the right to the left in order of increasing onsite Coulomb interaction U, there is an interchange of the energy order of the two resonances $\hbar\omega = \frac{1}{3}E_{1--}$ and $\hbar\omega = \frac{1}{2}E_{2+-}$, $\frac{1}{2}E_{1+-}$. The near coincidence of the triple and double resonances for the intermediate values of U creates the appearance of a strong single peak in Fig. 8a. For larger values of the onsite Coulomb interaction, the H_G and T_{1G} resonances split again and a weak T_{1G}-related peak occurs at the low-energy tail of the THG structure.

Our calculated spectrum can be used to infer the symmetry of two-particle elementary excitations observed experimentally. In the THG experiment[51,52] two peaks were observed at 1.3 μm and 1.06 μm. By taking a combination of relatively large parameters V, U, and $e^2/(\epsilon R_0)$, we can interpret the lower two-photon resonance to yield the measured energy of the H_G exciton at 1.9 eV and the higher triple-photon resonance to yield the energy of the T_{1U} exciton at 3.5 eV. A previous interpretation of the low-energy peak in the THG spectrum as a two-photon resonance with the one-photon forbidden T_{1G} level[51], even though in agreement with the low value of the resonance energy, could not explain the absence of the H_G exciton in the spectrum. We have demonstrated here that, with the help of a careful symmetry analysis, nonlinear optical spectroscopy can clarify the complicated electronic structure of the C_{60} molecule, especially its electron-hole pair excitations.

We note briefly that, in the case of the excitonic ground state T_{2G}, the interpretation of the THG would be different. According to the $\Delta L = \pm 1$ and $\Delta L = 0$ selection rules, a three-photon resonance excites the H_U or G_U exciton at $\hbar\omega = (E_{L--} - E_{3+-})/3$, $(L = 2, 3)$. Many transitions may contribute to the two-photon resonance. Among them are $H_U \to T_{1G}$, H_G, T_{2G}, and G_G, or $G_U \to H_G$, T_{2G}, and G_G.

V. DISCUSSIONS

In this paper, we address the issue of the strong electron correlation in a C_{60} molecule by an analytical model making maximum use of symmetry. The basic component is a simple quasi-particle model based on a tight-binding scheme of $\pi-$orbitals of the HOMO and LUMO states, with parameters deduced from photoemission and inverse photoemission experiments. The assumption of the closed-shell ground state is tested against the energies of the electron-hole pair excited states. The interaction between electrons and holes includes the Coulomb interaction of the $\pi-$orbitals on the same carbon atom and the long-range interaction between different carbon sites with a constant dielectric screening. The onsite electron-hole interaction is dominated by the exchange term, and is, therefore, repulsive while the electron-hole interaction on different carbon sites is attractive. The balance between these two terms depends, in our model, on the dielectric screening.

Our theory of the linear optical absorption spectra based on the closed-shell ground state agrees with experiment for a reasonably strong dielectric screening of the long-range interaction. We have established the relation between the energies or relative oscillator strengths of the dipole-active excitons and the Coulomb interaction terms connecting these excitons of the same symmetry. This coupling effect explains the observed strong T_{1U} exciton peaks in the linear optical absorption spectra. For the third-harmonic generation, our theory identifies the doublet excitation at the fundamental wavelength $\lambda \approx 1.3$ μm as the forbidden H_G exciton and not as the T_{1G} exciton suggested by experiment, whereas the triple resonance is clearly related to the T_{1U} excitation. This identification is supported by the argument invoking the approximate angular momentum selection rule in the nearly centrosymmetric molecule (see Sec. IV). The same transition to the H_G pairs is found to play a role if an external static electric field is applied to the C_{60} molecules. We predict a pronounced optical Kerr effect with a photon resonance at the H_G energy.

We wish to note an interesting scenario in which the closed-shell A_G state is unstable against an electron-hole pair excitation of symmetry T_{2G} with a reasonably weak dielectric screening. The consequences of having a T_{2G}

exciton state as the ground state are extraordinary. The optically dipole-allowed states are subsets of the H_U. The most interesting possibility is that a quasi-particle state now consists of an electron (or hole) plus an electron-hole pair, leading to strong correlation effects. Symmetry consideration would lead to more photoemission lines than the closed-shell ground state scenario. An experimental test of the electro-optic effect, which can discriminate the ground state symmetry, is described in Sec. IV.C.

A less extreme possibility is the small excitation energy of the T_{2G} exciton. The quasiparticle dynamics can be affected by the easy Coulomb excitations of such excitons. In particular, this could provide a source of effective quasiparticle interaction and, thus, possibly a source for superconductivity.

While our model study of the excitons has indicated that the most likely scenario of the ground state in C_{60} is the closed-shell A_G, it points out the possibility of constructing other molecular solids which lowers the excitonic states. The requirement is the strength of the inter-site electron-hole attraction over the onsite repulsion, which might be achieved by increasing the number of atom sites in a molecule. Our model approach may also be used to study excitons in quantum dots when the effective-mass approximation fails. We leave the investigation of the above conjectures to future work.

ACKNOWLEDGMENT

One of the authors (F.B.) gratefully acknowledges the kind hospitality of the University of California at San Diego. This work is financially supported by the Volkswagen Foundation and the National Science Foundation (NSF) (Grant No. INT-9513363, DMR-9421966, and DMR-9721444).

[1] H.W. Kroto, J.R. Heath, S.C. O'Brien, R.F. Curl, and R.E. Smalley, Nature (London) **318**, 162 (1985).

[2] A.F. Hebbard *et al.,* Nature (London) **350**, 600 (1991); K. Holczer et al., Science **252**, 1154 (1991); M.J. Rosseinsky et al., Phys. Rev. Lett. **66**, 2830 (1991); K. Tanigaki and others, Nature **352**, 222 (1991).

[3] P.-M. Allemand *et al.,* Science **253**, 301 (1991).

[4] R.W. Lof, M.A. van Veenendaal, B. Koopmans, H.T. Jonkman, and G.A. Sawatzky, Phys. Rev. Lett. **68**, 3924 (1992).

[5] B. Friedman and J. Kim, Phys. Rev. B**46**, 8638 (1992).

[6] J. Dong *et al.,* Phys. Rev. B **54**, 13611 (1996) and references therein.

[7] P.E. Lammert, D.S. Rokhsar, S. Chakravarty, S. Kivelson, and M.I. Salkola, Phys. Rev. Lett. **74**, 996 (1995). and references therein.

[8] R. Friedberg, T.D. Lee, and H.C. Ren, Phys. Rev. B**46**, 14150 (1992).

[9] S. Leach, M. Vervloet, A. Després, E. Breheret, J.P. Hare, T.J. Dennis, H.W. Kroto, R. Taylor, and D.R.M. Walton, Chem. Phys. **160**, 451 (1992).

[10] I. László and L. Udvardi, Chem. Phys. Lett. **136**, 418 (1987); J. Molecular Structure (Theochem.) **183**, 271 (1989).

[11] R.D. Bendale, J.D. Baker, and M.C. Zerner, Int. J. Quantum Chem. Symp. **25**, 557 (1991).

[12] F. Negri, G. Orlandi, and F. Zerbetto, J. Chem. Phys. **97**, 6496 (1992).

[13] F. Bechstedt, Adv. Phys. **32**, 161 (1992).

[14] E.L. Shirley and S.G. Louie, Phys. Rev. Lett. **71**, 133 (1993); S.G. Louie and E.L. Shirley, J. Phys. Chem. Solids **54**, 1767 (1993).

[15] S. Saito and A. Oshiyama, Phys. Rev. Lett. **66**, 2637 (1991).

[16] W.Y. Ching *et al.*, Phys. Rev. Lett. **67**, 2045 (1991).

[17] C.M. Varma, J. Zaanen, and K. Raghavachari, Science **254**, 989 (1991).

[18] M. Schlüter, Phys. Rev. Lett. **68**, 526 (1992).

[19] E.L. Shirley, L.X. Benedict, and S.G. Louie, Phys. Rev. B **54**, 10970 (1996).

[20] R.F. Curl and R.E. Smalley, Sci. Am. **265**, 32 (1991).

[21] R.C. Haddon, L.E. Brus, and K. Raghavachari, Chem. Phys. Lett. **125**, 459 (1986).

[22] D.A. Bochvar and E.G. Gal'pern, Dokl. Akad. Nauk SSSR [Chem.] **209**, 610 (1973).

[23] Y. Deng and C.N. Yang, Physics Letters A**170**, 116 (1992).

[24] L.J. Sham and T.M. Rice, Phys. Rev. **144**, 708 (1966).

[25] N. Laouini, O.K. Andersen, and O. Gunnarsson, Phys. Rev. B**51**, 17446 (1995).

[26] M. Hamermesh, *Group Theory and Its Application to Physical Problems* (Addison-Wesley, Reading, MA, 1962).

[27] D.A. Varshalovich, A.N. Moskalev, and V.K. Khersonskii, *Quantum Theory of Angular Momentum* (World Scientific, Singapore 1988).

[28] T. Takahashi *et al.,* Phys, Rev, Lett. **68**, 1232 (1992).

[29] J.H. Weaver *et al.,* Phys. Rev. Lett. **66**, 1741 (1991); J.H. Weaver, P.J. Benning, F. Stepniak, and D.M. Poirier, J. Phys. Chem. Solids bf 53, 1707 (1992).

[30] P.J. Benning, J.L. Martins, J.H. Weaver, L.P.F. Chibante, and R.E. Smalley, Science **252**, 1417 (1991).

[31] In the standard spectroscopic notation an additional upper index 2S+1, which gives the multiplicity of the states, is necessary for a complete characterization. However, in the considered case of singlet states ($S = 0$) the multiplicity is fixed to the value 1 and, hence, may be omitted.

[32] S. Ishibashi, N. Terada, M. Takumoto, N. Kinoshita, and H. Iharn, J. Phys. CM **4**, L169 (1992).

[33] P. Ecklung, Bull. Amer. Phys. Soc. **37**, 191 (1992); A.F. Hebard, R.C. Haddon, R.M. Fleming, and A.R. Kortan, Appl. Phys. Lett. **59A**, 2109 (1991).

[34] Y.-N. Xu, M.-Z. Huang, and W.Y. Ching, Phys. Rev. B**44**, 13171 (1991).

[35] Ph. Lambin, A.A. Lucas, and J.-P. Vigneron, Phys. Rev. B**46**, 1794 (1992).

[36] G. Cappellini, F. Bechstedt, A. Bosin, and F. Casula, Phys. Stat. Sol. (B) **189**, 1534 (1995).

[37] P.L. Hansen, P.J. Fallon, and W. Krätschmer, Chem. Phys. Lett. **181**, 367 (1991).
[38] C. Hartmann, M. Zigone, G. Martinez, E.L. Shirley, L.X. Benedict, S.G. Louie, M.S. Fuhrer, and A. Zettl, Phys. Rev. B**52**, R5550 (1995).
[39] Z. Gasyna, P.N. Schatz, J.P. Hare, T.J. Dennis, H.W. Kroto, R. Taylor, and D.R.M. Walton, Chem. Phys. Lett. **183**, 283 (1991).
[40] S.L. Ren, Y. Wang, A.M. Rao, E.McRae, J.M. Holden, T. Hager, KaiAn Wang, W.-T. Lee, H.F. Ni, J. Selegue, and P.C. Eklund, Appl. Phys. Lett. **59**, 2678 (1991).
[41] H. Ajie, M.M. Alvarez, S.J. Anz, R.D. Beck, F. Diederich, F. Fostiropoulos, D.R. Huffman, W. Krätschmer, Y. Rubin, K.E. Schriver, D. Sensharma, and R.L. Whetten, J. Phys. Chem. **94**, 8630 (1990).
[42] P.A. Heiney, J.E. Fisher, A.R. Mcghie, W.J. Romanow, A.M. Denenstein, J.P. McCauley, Jr., A.B. Smith, and D.E. Cox, Phys. Rev. Lett. **66**, 2911 (1991).
[43] R. Sachidanandam and A.B. Harris, Phys. Rev. Lett. **67**, 1467 (1991).
[44] W.I.F. David, R.M. Ibberson, J.C. Matthewman, K. Prassides, and others, Nature (London) **353**, 147 (1991).
[45] G.P. Banfi, D. Fortusini, M. Bellini, and P. Milano, Phys. Rev. B**56**, R10075 (1997).
[46] F.P. Strohkendl, R.L. Larsen, T. Axenson, R.L. Dalton, R.W. Hellwarth, H. Sarkas, and Z.H. Kafafi, Proc. SPIE **2854**, 191 (1996).
[47] B. Koopmans, A.-M. Janner, H.T. Jonkman, G.A. Sawatzky, and F. van der Woude, Phys. Rev. Lett. **71**, 3569 (1993).
[48] A.-M. Janner, R. Eder, B. Koopmans, H.T. Jonkman, and G.A. Sawatzky, Phys. Rev. B**52**, 17158 (1995).
[49] J.A. Armstrong, N. Bloembergen, J. Ducuing, and P. Pershan, Phys. Rev. **127**, 1918 (1962).
[50] See, for example, Th. Östreich, K. Schönhammer, and L.J. Sham, Phys. Rev. Lett. **74**, 4698 (1995).
[51] F. Kajzar, C. Taliani, R. Danielli, S. Rossini, and R. Zamboni, Chem. Phys. Lett. **217**, 418 (1994).
[52] F. Kajzar, C. Taliani, R. Zamboni, S. Rossini, and R. Danielli, SPIE **2025**, 352 (1993).

FIG.1: The structure of the C_{60} molecule. Each dot denotes the position of a carbon atom. The connecting solid lines indicate the bonds. The intact icosahedron with the vertices at N, S, A_i, and A_i' $(i = 1, \ldots, 5)$ is indicated by the dashed lines.

FIG.2: Schematic four-level diagram of HOMO and LUMO states for characterization of the lowest electronic excitations in the C_{60} molecule.

FIG.3: Feynman diagrams for the electron (upward arrows) - hole (downward arrows) interaction (dashed line): (a) the direct attraction, (b) the exchange counterpart.

FIG.4: The excitation energies of Frenkel excitons belonging to the single-particle pairs $h_u \to t_{1u}$, $h_u \to t_{1g}$, $h_g \to t_{1u}$, and $h_g \to t_{1g}$ versus the effective interatomic Coulomb interaction strength $e^2/(\epsilon R_0)$. The intraatomic Coulomb interaction is fixed at two values (a) $U = 0$ and (b) $U = 4V$. T_{1P}: solid line, H_P: dashed line. Both parities $P = +, -$ are considered. The high-energy (low-energy) solutions of the coupled pairs $\Lambda = +$ $(\Lambda = -)$ are plotted as thick (thin) lines. All energies are given in units of the hopping parameter V.

FIG.5: The lowest even-parity exciton energies versus the interatomic Coulomb interaction. The zero line is given by the closed-shell Hartree-Fock ground state. (a) $U = 0$, (b) $U = 4V$.

FIG.6: Absorption spectra of C_{60} versus the photon energy in units of V for different parameters of the effective Coulomb interaction and damping parameters Γ. Solid line: $U = 3V$, dashed line: $U = 2V$, dotted line: $U = V$, dash-dotted line: $U = 0$. The ratio of the intersite and intrasite Coulomb interaction is fixed to $e^2/(\epsilon R_0 U) = 0.2377$ (left panel) and 0.0517 (right panel).

FIG.7: Absorption spectra of C_{60} molecules in a static electric field versus the photon energy near the forbidden transition $h_u \to t_{1u}$ for different parameters of the effective Coulomb interaction. Solid line: $U = 3V$, dashed line: $U = 2V$, dotted line: $U = V$, dash-dotted line: $U = 0$. (a) $e^2/(\epsilon R_0 U) = 0.2377$, (b) $e^2/(\epsilon R_0 U) = 0.0517$. The damping parameter is chosen as $\Gamma = 0.05V$. Each spectrum has to be multiplied with the prefactor $(eFR_0/2V)^2$ to compare with the strength in Fig. 6.

FIG.8: Spectral variation of the THG susceptibility in the region of the lower 3-photon T_{1U} and 2-photon H_G resonances for the same parameters of the effective Coulomb interaction as in Fig. 7. The damping parameter is chosen as $\Gamma = 0.03V$ for both allowed and forbidden excitons.

Table I. The intraatomic and interatomic Coulomb interaction matrix elements (3.11, 3.12, 3.13).
(I.R. — Irreducible representation)

I.R.	Quantum numbers			$F_{pp'}(LNP)$			$H_{pp'}(LNP)$			$X_{pp'}(LNP)$		
	L	N	P	$++$	$--$	$+-$	$++$	$--$	$+-$	$++$	$--$	$+-$
T_{1G}	1	0,±1	1	0.50000	0.76690	0.61923	0.87251	0.89689	0.22713	-0.02111	-0.03239	-0.02615
H_G	2	0,±1,±2	1	1.50000	1.23310	0.79877	0.85182	0.82745	0.05389	0.03329	0.04047	0.05790
T_{2G}	3	0,±3	1	1.33333	1.99975	-1.63289	0.85527	0.87308	-0.09762	-0.08122	-0.12181	0.09947
G_G	3	±1,±2	1	0.50000	0.13364	-0.23822	0.87251	0.87134	-0.16449	-0.00908	-0.00303	0.00416
T_{1U}	1	0,±1	-1	1.54204	1.50000	1.50777	0.85363	0.84560	0.19439	0.16148	0.11124	0.13512
H_U	2	0,±1,±2	-1	0.45796	0.50000	-0.08977	0.87070	0.87873	0.08662	-0.01309	-0.02673	0.00445
T_{2U}	3	0,±3	-1	0.63864	1.00000	0.21489	0.86786	0.91547	-0.18339	0.02377	-0.01409	0.01251
G_U	3	±1,±2	-1	1.54204	1.25000	-1.17978	0.85363	0.81391	-0.11652	-0.06371	-0.07559	0.07082

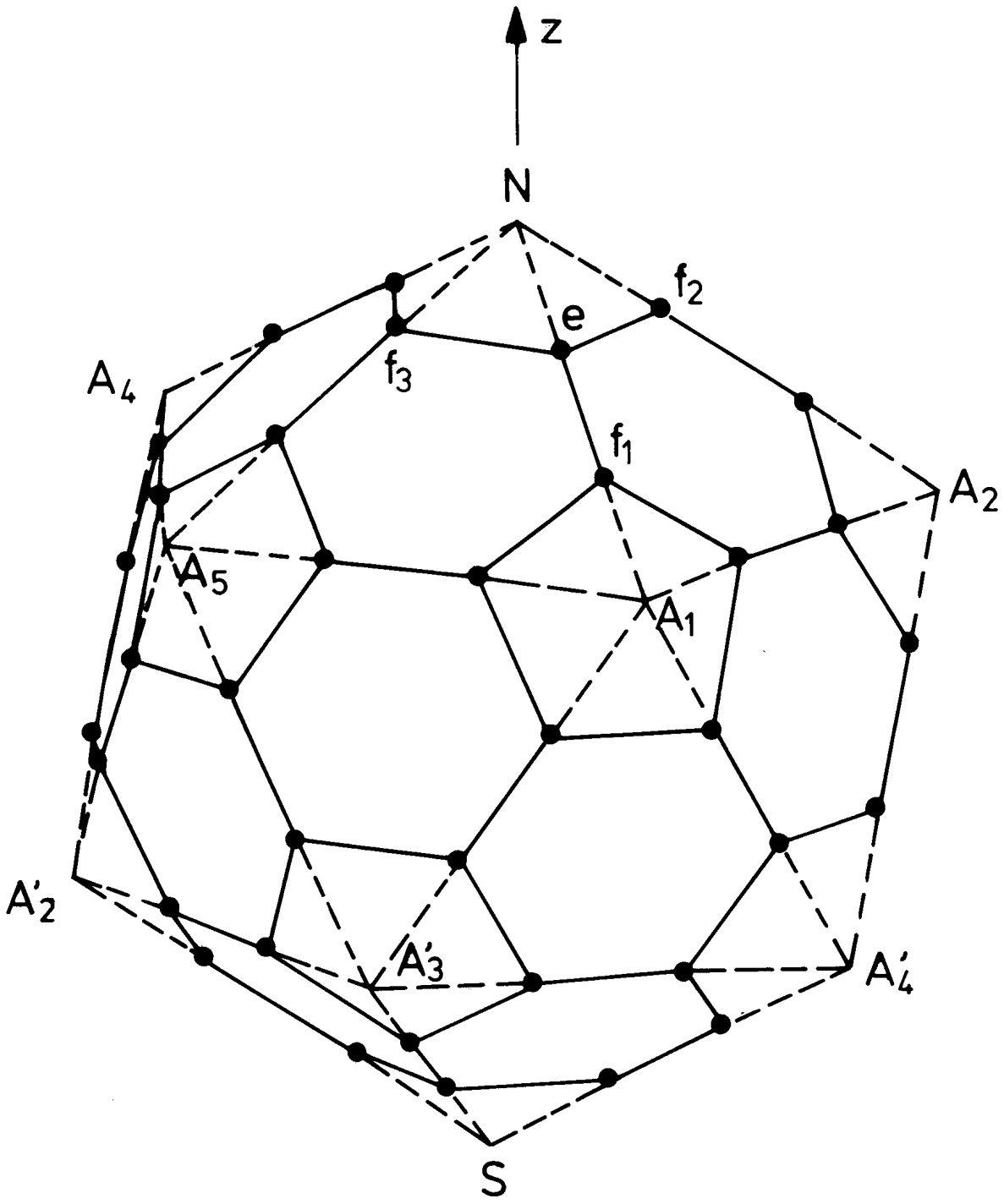
z
N
e
f_2
f_3
A_4
f_1
A_2
A_5
A_1
A'_2
A'_3
A'_4
S

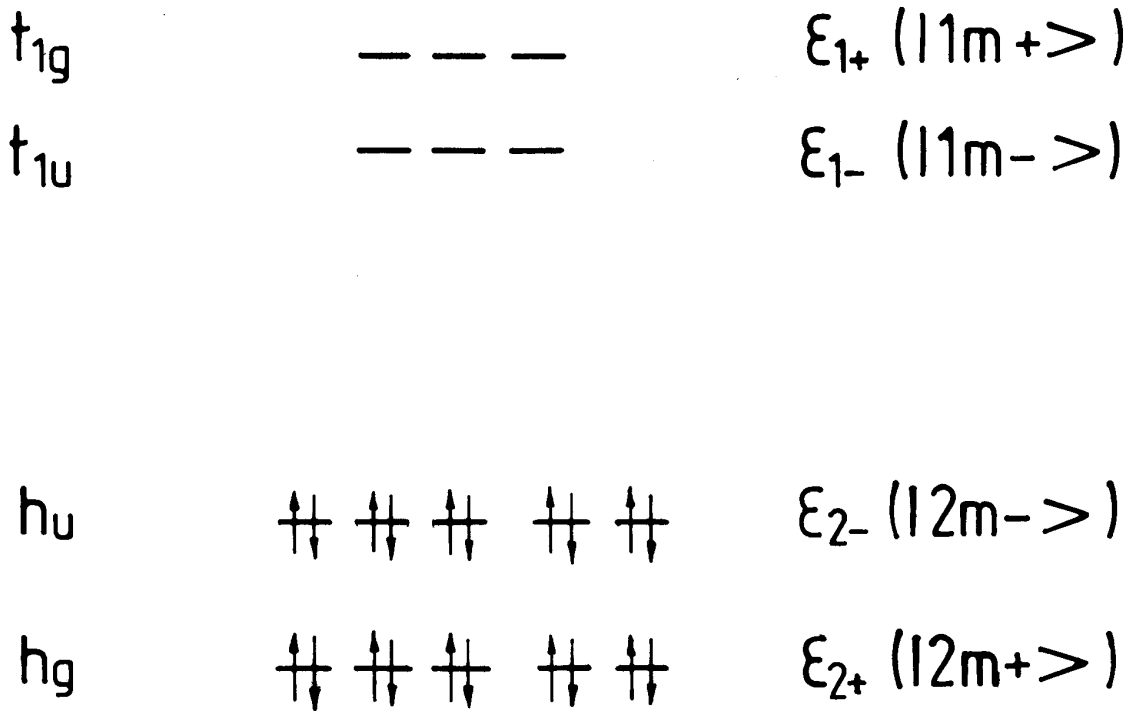
t_{1g}
t_{1u}
ε_{1+} (11m+>)
ε_{1-} (11m->)
h_u
h_g
ε_{2-} (12m->)
ε_{2+} (12m+>)

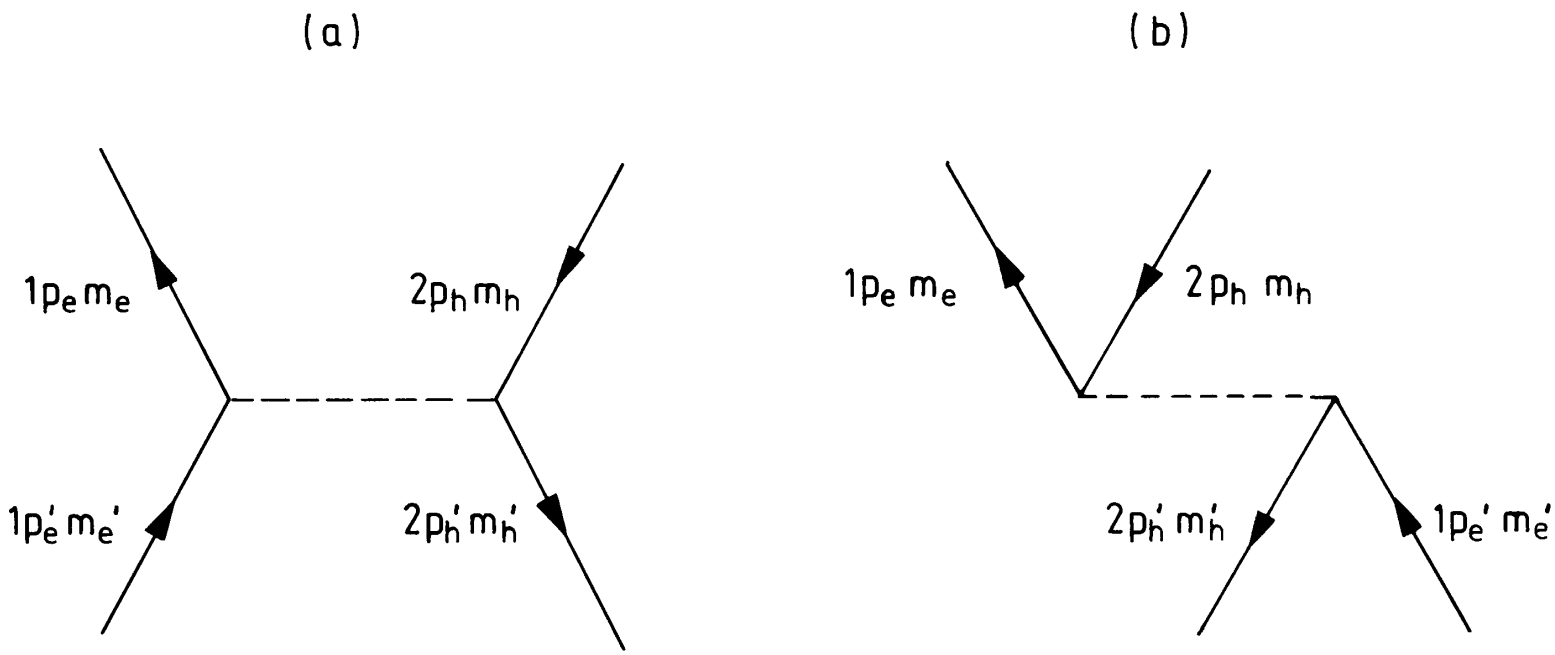
(a)
1p_e m_e
2p_h m_h
1p_e' m_e'
2p_h' m_h'
(b)
1p_e m_e
2p_h m_h
2p_h' m_h'
1p_e' m_e'

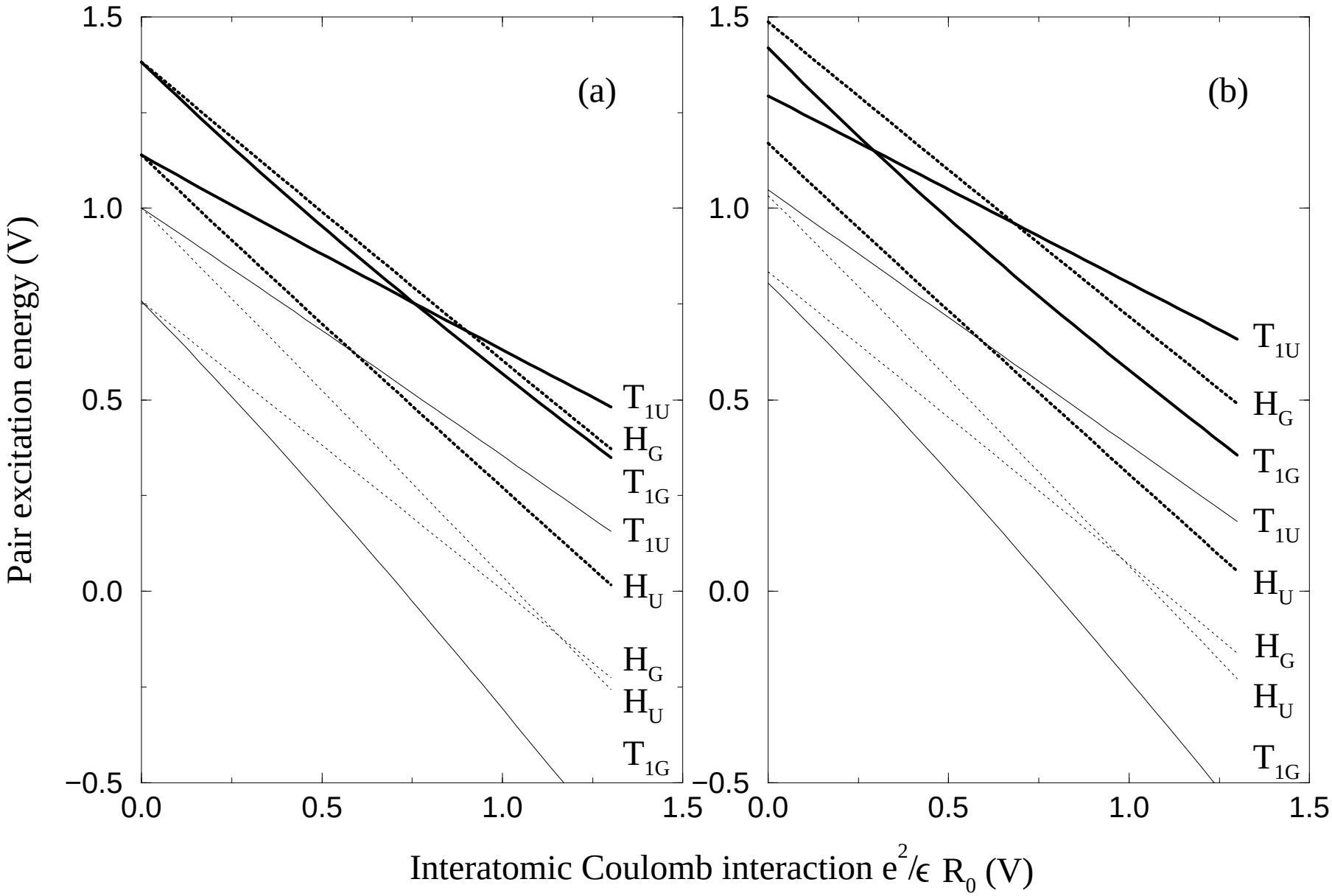
(a)
(b)
Pair excitation energy (V)
Interatomic Coulomb interaction e²/ϵ R₀ (V)
1.5
1.0
0.5
0.0
−0.5
0.0
0.5
1.0
1.5
T1U
HG
T1G
T1U
HU
HG
HU
T1G
T1U
HG
T1U
HU
HG
HU
T1G

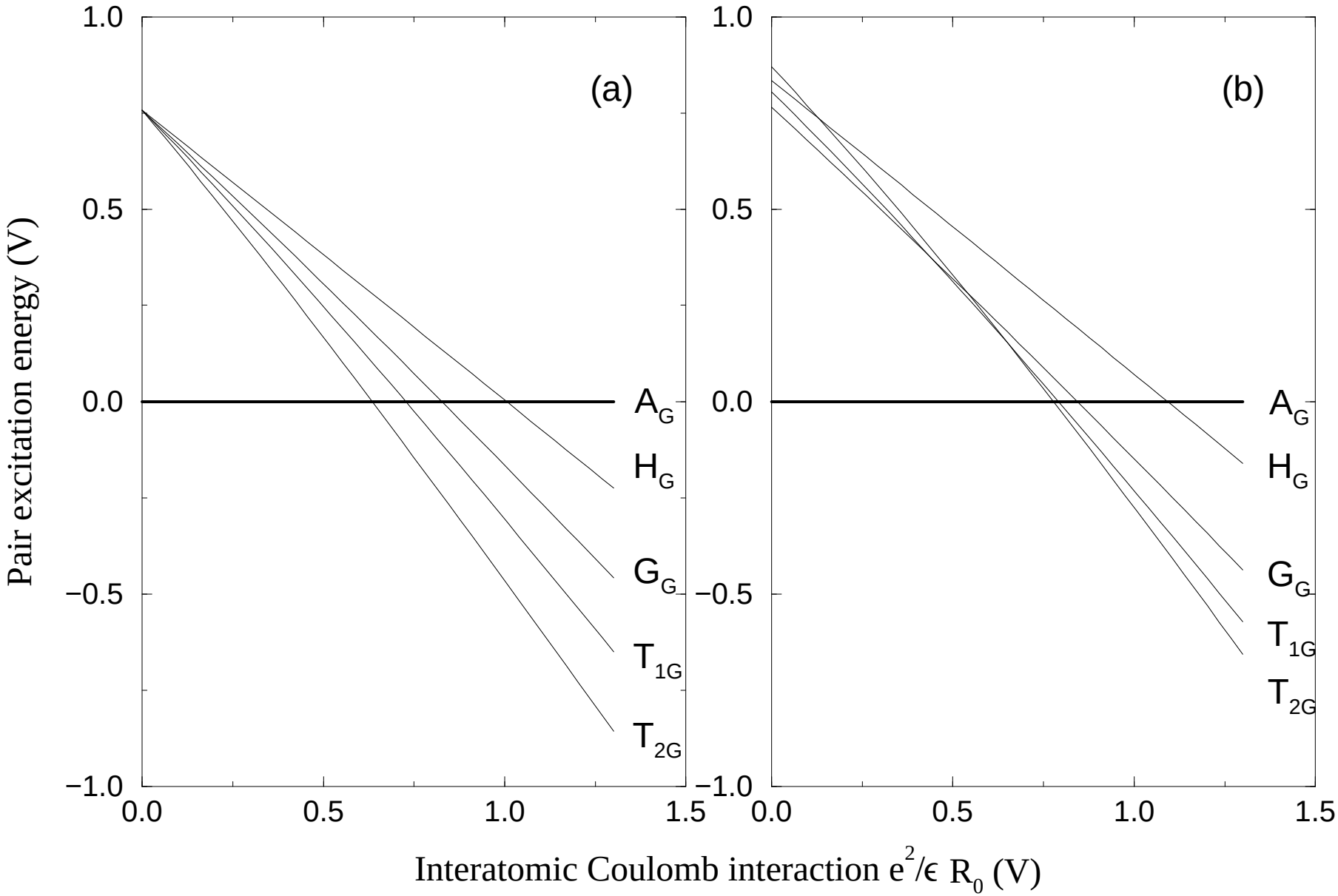
(a)
(b)
Pair excitation energy (V)
Interatomic Coulomb interaction e²/ϵ R₀ (V)
1.0
0.5
0.0
−0.5
−1.0
0.0
0.5
1.0
1.5
A_G
H_G
G_G
T_1G
T_2G

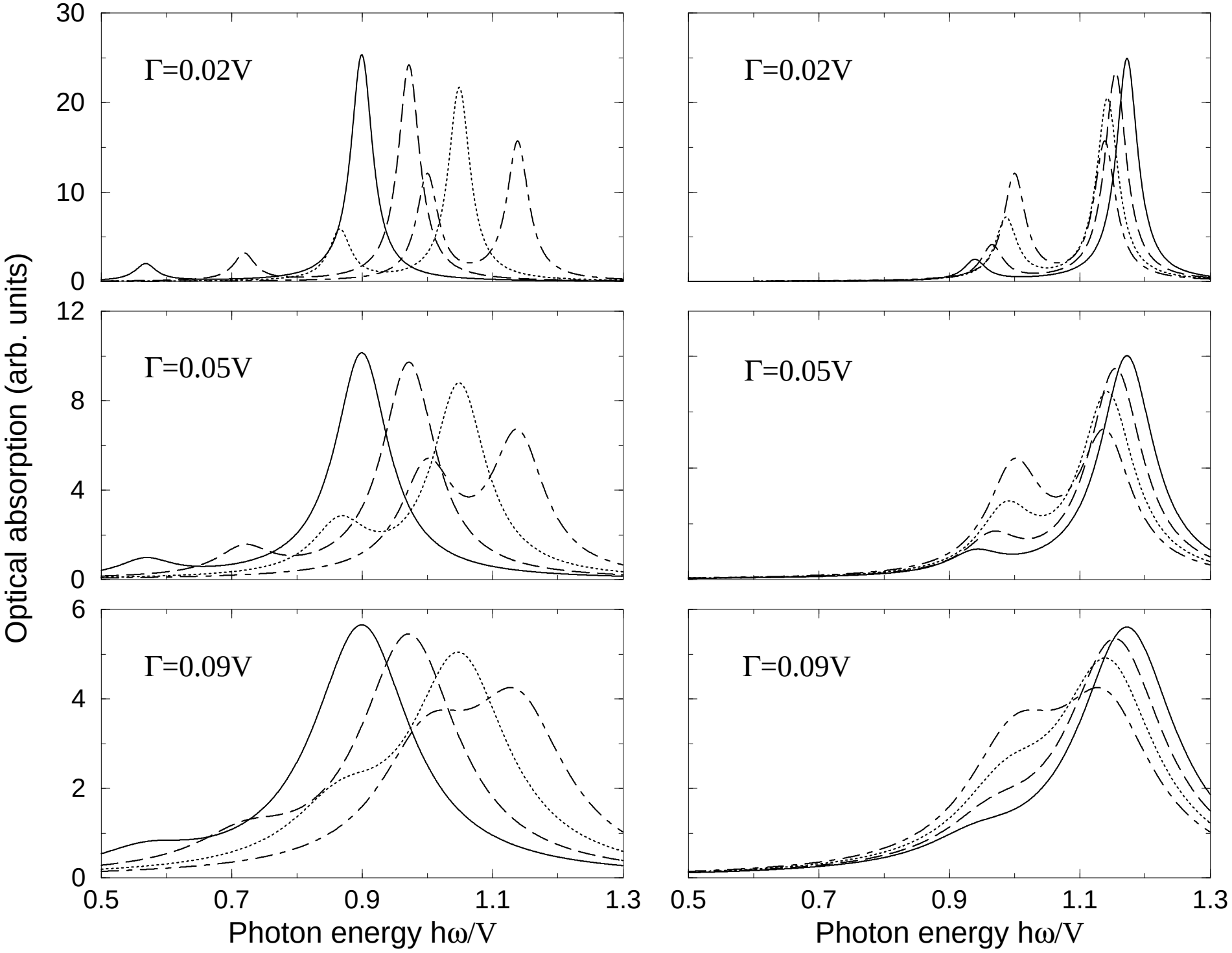
Γ=0.02V
Γ=0.02V
Γ=0.05V
Γ=0.05V
Γ=0.09V
Γ=0.09V
Optical absorption (arb. units)
Photon energy hω/V
Photon energy hω/V
0
10
20
30
0
4
8
12
0
2
4
6
0.5
0.7
0.9
1.1
1.3

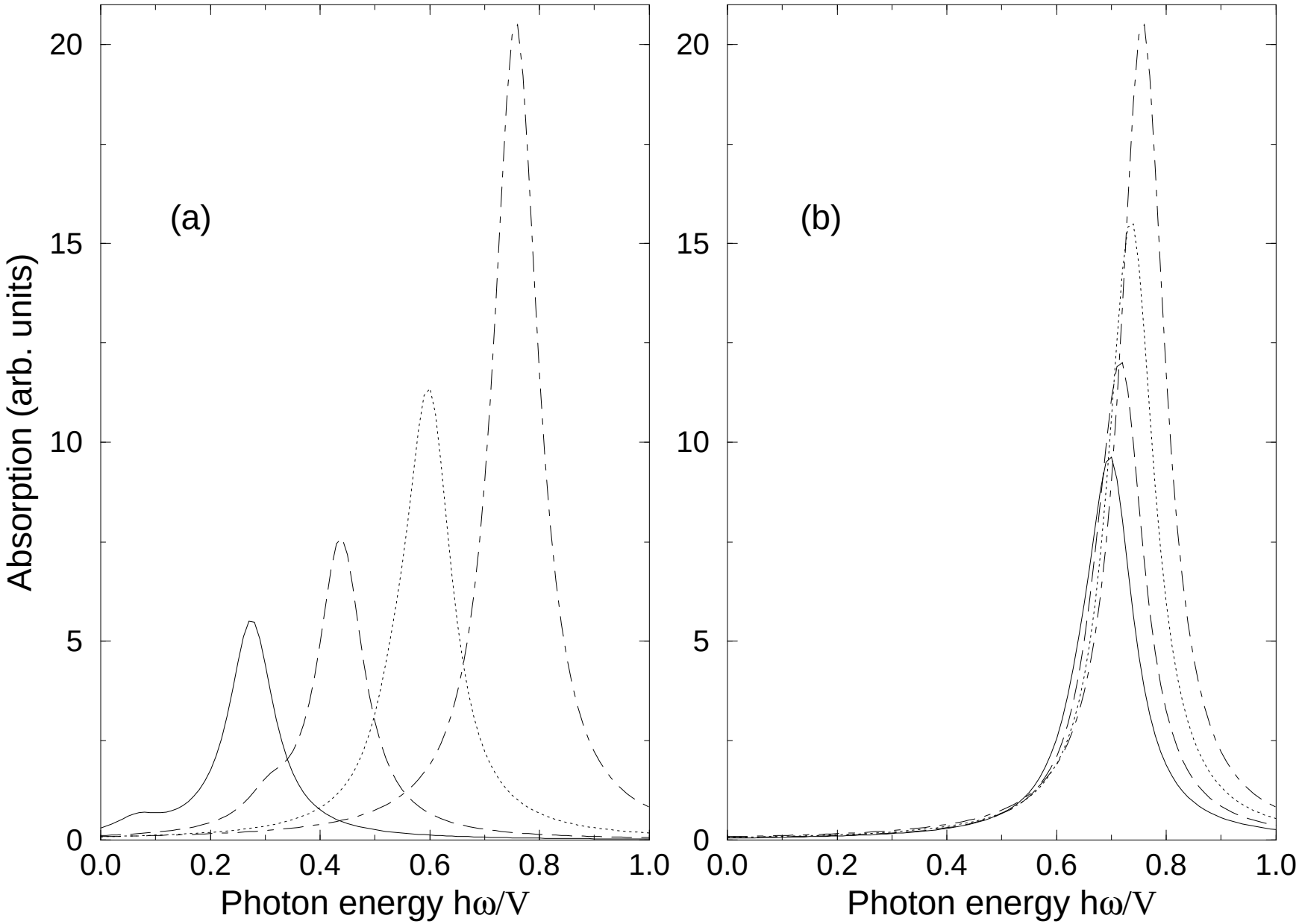
(a)
(b)
Absorption (arb. units)
Photon energy hω/V
Photon energy hω/V
0
5
10
15
20
0.0
0.2
0.4
0.6
0.8
1.0

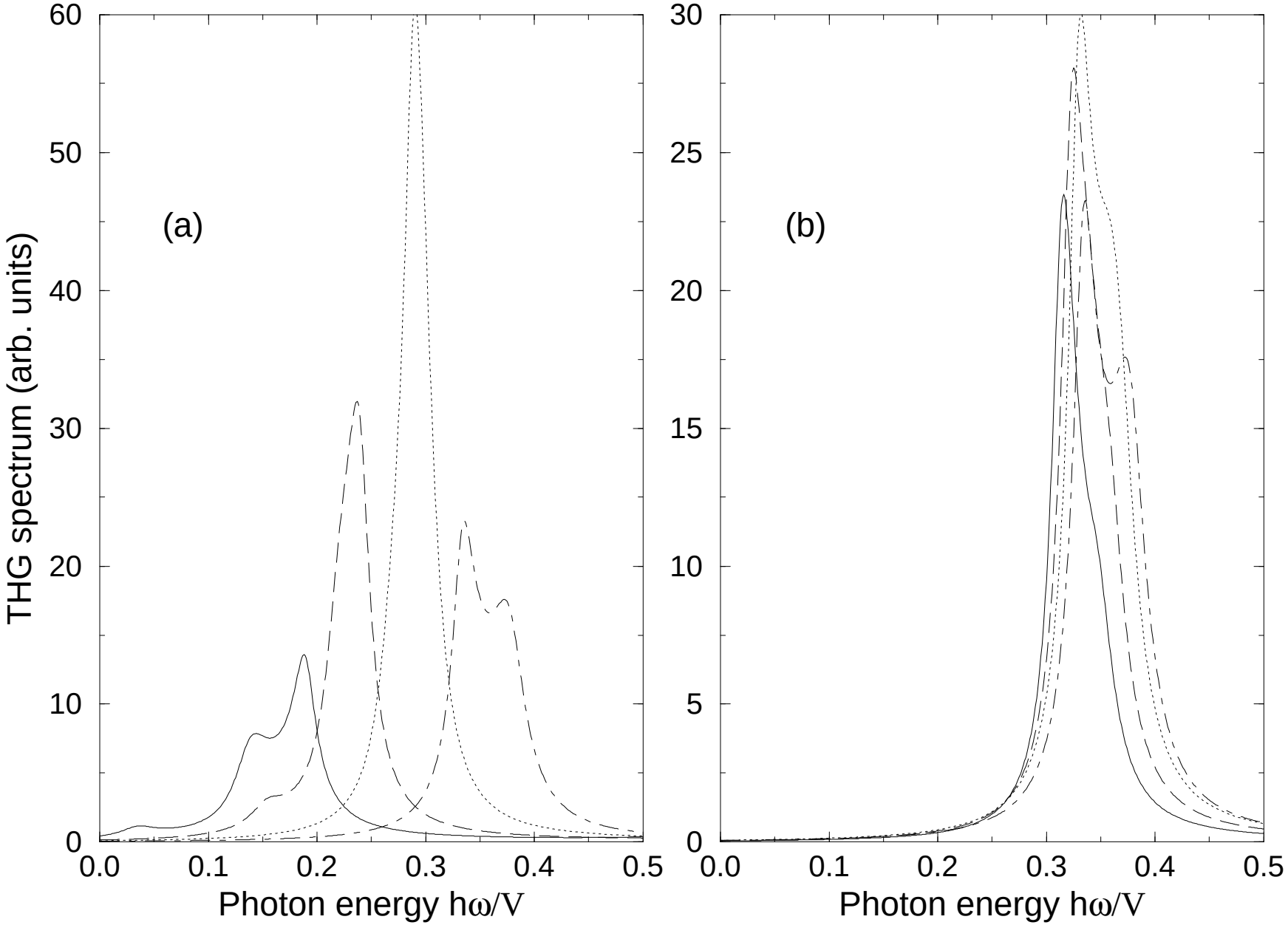
(a)
(b)
THG spectrum (arb. units)
Photon energy hω/V
Photon energy hω/V
0
10
20
30
40
50
60
0
5
10
15
20
25
30
0.0
0.1
0.2
0.3
0.4
0.5